Efficient Recombinant Production and Functional Characterisation of Cytotoxic and Haemotoxic Snake Venom Metalloproteinases

Authors:

Sophie Hall[1], Iara Aimê Cardoso[1], Mark C. Wilkinson[2], Maria Molina Carretero[3], Srikanth Lingappa[1], Bronwyn Rand[1], Dakang Shen[1], Johara Boldrini-França[1], Richard Stenner[1], Georgia Balchin[1], Konrad Kamil Hus[1,4], Renaud Vincentelli[5], Andrew Mumford[3], Nicholas R. Casewell[2], Imre Berger[1,6], Christiane Schaffitzel[1]

Affiliations:

[1] School of Biochemistry, University of Bristol, University Walk, Bristol BS8 1TD, UK

[2] Centre for Snakebite Research and Interventions, Liverpool School of Tropical Medicine, Liverpool L3 5QA, UK

[3] School of Cellular and Molecular Medicine, University of Bristol, 1 Tankard's Close, Bristol BS8 1TD, UK

[4] Department of Biotechnology and Bioinformatics, Faculty of Chemistry, Rzeszow University of Technology, Powstancow Warszawy 6, 35-959 Rzeszow, Poland

[5] Architecture et Fonction des Macromolécules Biologiques (AFMB), UMR 7257 CNRS-Aix-Marseille Université, 13288 Marseille, France

[6] Max Planck Bristol Centre for Minimal Biology, School of Chemistry, University of Bristol, Cantock's Close, Bristol BS8 1TS, UK

Correspondence:

Christiane Schaffitzel, email: Christiane.berger-schaffitzel@bristol.ac.uk

Imre Berger, email: imre.berger@bristol.ac.uk

ABSTRACT

Snake venoms contain variable mixtures of toxins that evolved to incapacitate prey but cause extensive pathology in snakebite patients. In viper venom, the most potent toxins are the haemorrhagic and coagulopathic snake venom metalloproteinases (SVMPs). SVMP research has been hampered by the lack of an efficient generic recombinant production protocol. Using baculovirus/insect cell expression, we produced and functionally validated enzymes from all three structurally variable SVMP classes (PI, PII and PIII). Incorporating the native N-terminal prodomain, which blocks the active site via a cysteine-switch motif, overcame the cytotoxicity of SVMPs. Incubation with Zn^{2+} activated the SVMP zymogens, resulting in proteolysis of the PIII prodomain. Functional validation of the recombinant SVMPs was performed using protein substrate degradation, platelet aggregation and blood coagulation assays, benchmarked to native venom-purified SVMP. Our study provides a potent generic platform for the expression of SVMPs of value, for bioprospecting and discovery of novel snakebite therapeutics.

INTRODUCTION

Snakebite envenoming (SBE) affects 1.8 – 2.7 million people each year resulting in more than 100,000 deaths and 400,000 cases of morbidity[1]. Although 6.85 billion people live in areas with venomous snakes[2], SBE disproportionately affects the most economically disadvantaged areas of tropical and sub-tropical Latin America, sub-Saharan Africa and Asia[3], where access to healthcare is often limited. Consequently, SBE was designated a Category A Neglected Tropical Disease in 2017 by the World Health Organisation[1].

Snake venom is a complex cocktail of more than 100 proteins and peptides belonging to various toxin families[3]. While these toxin families vary extensively in terms of numbers and abundance of isoforms across different venomous snakes, the snake venom metalloproteinases (SVMP) are a pathologically important toxin family present in almost all snake venoms. These toxins play a significant role in the physiological effects resulting from both local and systemic envenoming, such as haemorrhage, coagulopathy and tissue necrosis[4]. In many medically important viperid snake genera, such as *Echis* (saw-scaled vipers), SVMP toxins are the most abundant toxin constituents, on average accounting for 33% of all toxins, though this can be as high as 72% in *Echis ocellatus*[5-7] (Fig. 1a).

SVMPs are complex, structurally variable, cysteine-rich, Zn^{2+}-dependent metalloproteinases that can be classified into three sub-classes based on domain architecture: PI (metalloproteinase domain only), PII (metalloproteinase and disintegrin domains) and PIII (metalloproteinase, disintegrin-like and cysteine-rich domains) (Fig. 1b); representatives of all three sub-classes are present in viper venom.

SVMPs are particularly toxic proteins with a wide range of substrates. They are known to degrade the basement membrane and extracellular matrix proteins, as well as several blood clotting factors, most notably fibrinogen, through their metalloproteinase domain[8]. Additionally, several SVMPs are known to activate blood clotting factors such as factor II (prothrombin) and X[9]. A loss in blood capillary wall integrity results in vascular leakage, resulting in both local and systemic haemorrhage[10]. Extracellular matrix breakdown also furthers the spread of other toxins, including phospholipases A2 and snake venom serine proteases[11]. In PII

SVMPs, the disintegrin domain contains a charged, integrin-binding motif, most commonly an arginine-glycine-aspartate (RGD) motif, which binds, among others, the fibrinogen receptor integrin $\alpha_{IIb}\beta_3$ [12], causing inhibition of platelet aggregation. The disintegrin domain can also inhibit angiogenesis through interference with integrins such as $\alpha_V\beta_3$ [13].

Because viper SVMPs often target components of the coagulation cascade with unique specificity and/or lack of reliance on typically essential co-factors, these enzymes are highly valuable for investigating and monitoring the treatment of pathologies related to haemostasis (e.g. factor deficiencies, bleeding disorders)[14]. In the clinic, the SVMPs RVV-X and ecarin are both used as standards for coagulation tests[15]. In addition, SVMP-derived disintegrins have been repurposed for use as, or inspiration for the design of, anti-platelet therapies to treat atherothrombosis in the form of unstable angina and myocardial infarction[3]. Thus, a single snake venom toxin family has yielded several translationally valuable tools for diagnosis and treatment of human disease. However, further exploitation of SVMPs is hampered by the considerable challenge in purifying individual SVMP proteins from venom, and the lack of robust, scalable, recombinant toxin production protocols, representing a bottleneck.

Currently, SVMPs are typically purified from venom by size exclusion chromatography (SEC), followed by ion exchange chromatography (IEX) of the peaks containing SVMPs. Further separation can be achieved by hydrophobic interaction chromatography (HIC) or reversed-phase high performance liquid chromatography (RP-HPLC)[16,17]. However, complete separation of endogenous functionally active SVMPs is difficult to achieve, because: (1) many venoms contain multiple related SVMP isoforms that share similar physicochemical properties, (2) the resulting yields of each particular isoform can be low, and (3) the use of some desirable separation approaches (e.g. RP-HPLC) can result in protein denaturation. Importantly, this procedure is impeded by limited access to sufficient amounts of extracted snake venom.

Recombinant expression of SVMPs could resolve the bottleneck, but proved difficult due to their cytotoxicity, domain complexity and high number of cysteine residues - for example, the PIII SVMPs contain between 20 and 40 cysteines[18]. Currently, protocols are available for the production of only a select few specific SVMPs

(including albocollagenase, bothropasin and ecarin)[19-21]. However, these suffer from limitations such as low yield and inactive proteins. Zymogen production of SVMPs has also been described, but it remains generally unknown how the zymogen is processed into the mature, active SVMP. Current protocols describe incubation of the zymogen for >7 days[21], incubation with other active proteinase toxins[22], or the insertion of a TEV protease cleavage site into the SVMP amino acid sequence[23]. However, a protocol to access functional PI, PII and PIII SVMPs in the quality and quantity required, has remained elusive to date.

Here, we established an efficient, generic protocol for recombinant production of SVMPs using the MultiBac baculovirus/insect cell expression system[24]. The MultiBac system is well-established for secretion of proteins, including the C-terminal heavy chain domain of the highly toxic protein, clostridial botulinum neurotoxin[25]. We reasoned the system would be highly suitable for SVMP production because (1) protein folding will be supported by eukaryotic, endogenous chaperones present in insect cells and (2) secreted proteins will undergo cellular protein quality control in the endoplasmic reticulum (ER) and Golgi apparatus for disulphide bond formation and glycosylation before secretion, ensuring that the toxins produced are correctly folded, soluble and authentically modified. Using a novel zymogen expression and activation strategy to overcome toxin cytotoxicity, we show that baculovirus/insect cell expression is suitable for routinely producing high quantities of active SVMPs.

Using this approach, we demonstrate successful expression and purification of representatives of all three structural subclasses, PI and PII SVMPs from *Echis ocellatus* and a PIII SVMP from *Echis carinatus sochureki* (Fig. 1c). We show successful purification and activation of the SVMPs, and characterise their activity *in vitro* using established casein[26], fibrinogen[26], fluorogenic peptide[27] and insulin degradation[16] assays. We further analysed the cytotoxicity and haemotoxicity of the recombinant SVMPs. For the PI SVMP, we show that the activity of recombinant SVMP is identical to that of the corresponding toxin purified from venom, compellingly validating the utility of our strategy. Our generic SVMP production protocol thus paves the way to systematically characterize SVMPs and unlock biomedical applications, in haematology, thrombosis and inflammation research and as targets for the discovery of novel snakebite therapeutics.

RESULTS

Recombinant SVMP expression

For our expression tests, we chose PI, PII and PIII SVMPs which, according to transcriptomics[28], are highly expressed in the venom gland of medically important vipers in Sub-Saharan Africa. We generated baculovirus/insect cell expression constructs for Q2UXQ3 (PI), A0A3G1E3U2 (PII) and E9JG34 (PIII), each encoding a melittin signal sequence for secretion, the toxin of interest and C-terminal tandem hexahistidine- and Avi-tags[29], codon optimised for both *Spotoptera frugiperda* and *Trichoplusia Ni* as expression hosts. Initially, recombinant production of mature SVMPs, without the N-terminally fused prodomain, was attempted (Fig. 2a-c). Protein expression yields, however, were extremely low, primarily due to SVMP cytotoxicity causing cell death immediately upon baculoviral infection. This was evidenced by very low cell viability, with more than 60% of cells dying within 72 hours of expression, and 100% cell death by 96 hours into the expression for the PI and PIII SVMPs (Fig. 2a). Yellow fluorescent protein (YFP) is used in the MultiBac expression system as an indicator of baculovirus performance and a proxy for heterologous protein production[24]. Typically, YFP fluorescence is followed during expression and cells/proteins are harvested when YFP production reaches a plateau[24]. Throughout mature SVMP expression, YFP fluorescence remained very low, consistent with pervasive premature cell death caused by the SVMP toxin resulting in low YFP production, and cell lysis leading to release of YFP into the media (Fig. 2b). Additionally, the decrease in YFP readings observed (days 3-5 after proliferation arrest) during expression could also be due to proteolytic degradation of YFP by the mature, active SVMP.

Western blot analysis detecting the His-tag fused C-terminally to the SVMP, showed that the mature PI and PIII had been successfully expressed within the cells. It also indicated that these SVMPs were soluble because they could be detected not only in the whole cell extract (SNP; combined supernatant/pellet) but also in the cleared lysate (SN; supernatant) (Fig. 2c). However, no SVMP was detected in the media sample in the Western blot, indicating that little or no SVMP had been secreted. This is possibly due to the death and lysis of the cells, caused by the toxin, impairing the secretion machinery before noticeable secretion had occurred. Taken together, expression of mature SVMPs detrimentally affects cell integrity, damaging the cells

very early after baculovirus infection as soon as protein production initiates, underscoring the toxicity of the SVMPs.

Therefore, subsequent expression strategies to produce SVMPs were aimed at inactivating the metalloproteinase. We first tested Marimastat, a broad-spectrum metalloproteinase inhibitor[30]. Marimastat binds to the active site of the metalloproteinase mimicking the structure of a peptide substrate, inhibiting SVMP activity[30]. During baculovirus infection, Marimastat was added to the medium at a final concentration of 3 µM and 6 µM, respectively (Supplementary Fig. 1a). At these concentrations however, Marimastat could not prevent cell death induced by PIII SVMP expression. On the contrary, the cell viability in the presence of 3 µM and 6 µM Marimastat was even further decreased. Additionally, less SVMP was detected in anti-His-tag Western blots in whole cell extract (SNP) and cleared lysate (SN), compared to the expression of mature SVMP without Marimastat (Fig. 1c, Supplementary Fig. 1a). Thus, Marimastat itself appears to be toxic to insect cells at the doses tested, and has no positive effect on SVMP expression and recovery.

Next, we tested SVMP active site mutants based on a previous report of an inactive PII SVMP purified from *Bothriechis lateralis* venom[31]. Two active site mutations were identified in the protein rendering it inactive (canonical sequence: HEXXHXXGXXH, inactive sequence: H**D**LGHNL**C**IDH). We inserted these mutations into our PI and PIII SVMPs. We found improved cell viability and detected elevated YFP signal for the PI SVMP active site mutant (Supplementary Fig. 1b). However, the PIII SVMP active site mutant still showed significant toxicity, reducing YFP levels as well as cell viability. Nonetheless, we successfully purified both PI and PIII SVMP active site mutants from the media using immobilised metal affinity purification (IMAC) via the oligohistidine tags present in our proteins. Based on our observations with the active site mutants, we concluded that inhibition of metalloproteinase activity during SVMP protein production has a positive effect, indicating that expressing inactivated SVMPs could be a viable, although inefficient, approach.

In the snake venom gland, SVMPs are produced with an N-terminally fused prodomain that is removed through autocleavage during post-translational processing of the protein (Fig. 2d). The prodomain comprises a small, highly conserved propeptide sequence (usually PKMCGVT) - this propeptide acts as a cysteine switch to maintain enzyme latency[32]. AlphaFold 2[33] predicts that the

prodomain adopts a β-barrel structure and folds around the metalloproteinase (MP) domain, slotting the propeptide into the active site of the MP domain, where the propeptide cysteine co-ordinates the active site Zn^{2+} ion, along with the three active site histidines (Fig. 2d). This renders the MP inactive as the Zn^{2+} ion cannot be accessed by substrates in the active site. Inspired by this, we designed propeptide-SVMP fusion proteins using the propeptide responsible for the cysteine switch, PKMCGVT. We fused three propeptide repeats to the N-terminus of the SVMP followed by a TEV protease cleavage site. We hypothesised that this would increase the avidity of the propeptide to the MP active site and efficiently inactivate the enzyme. Cell viability for the propeptide-SVMP fusion expression trials were higher at days 3-5 when compared to the mature SVMPs (Fig. 2a and 2e). However, towards the end of expression less than 25% of cells were left alive (day 5), likely limiting protein secretion. Although YFP fluorescence levels for PI and PIII had slightly increased (Fig. 2f) compared to expression of the mature SVMP (Fig. 2b), YFP expression was still significantly lower as compared to a positive control which expressed an unrelated, non-toxic protein. Western blot analysis confirmed PI and PIII SVMPs were expressed and soluble (Fig. 2g). However, propeptide-SVMP fusion protein yields in the media still remained too low to progress to purification.

Next, we tested expression of complete SVMP zymogens, where the entire prodomain including propeptide is fused N-terminally to the MP domain (Fig. 2d) adopting a compact structure as predicted by AlphaFold 3[34] with high inter-chain predicted Template Modelling (ipTM) and predicted TM scores (Supplementary Fig. 2). Cells expressing PI, PII and PIII SVMPs as zymogens showed clearly improved cell viability, remaining above 60% on day 4 of expression (Fig. 2h). PIII SVMP zymogen was harvested on day 4 to avoid further cell death and lysis. In contrast, the cells expressing PI and PII SVMPs remained ~75% viable on day 5 of expression when the SVMPs were harvested. Notably, the zymogen-expressing cells had considerably higher YFP readings as compared to the cells previously expressing mature PI and PIII SVMPs, and no loss of YFP fluorescence over time was observed (Fig. 2i). Western blot analysis confirmed the presence of PI, PII and PIII zymogens in cell extract and lysate; and a band was also detected in the media fraction, indicating successful secretion (Fig. 2j). We conclude that SVMPs require the full-length N-terminally fused prodomain to ensure enzyme latency is maintained, and to

allow for significant amounts of protein to be produced and secreted when recombinantly expressed using a baculovirus/insect cell system.

Purification of SVMP zymogens

Following secretion of the SVMPs into the media, a three-step purification was performed. Firstly, cells were pelleted by centrifugation, and the media containing secreted SVMPs was passed through a HiTrap IMAC column for metal affinity purification to enrich the secreted protein from the comparatively large culture media volume. SVMPs were eluted using imidazole. Fractions containing SVMP zymogen were dialysed and further purified by anion exchange chromatography (IEX), followed by size exclusion chromatography (SEC). SVMP zymogens generally eluted in one prominent peak in SEC (Fig. 3).

Notably, dialysis following IMAC affinity purification of PI SVMP resulted in self-cleavage of the zymogen as evidenced by a downward shift of the PI protein band in the SDS gel from 55 kDa to 45 kDa before and after dialysis, respectively (Supplementary Fig. 3a). Western Blot analysis indicated a loss of the His-tag after dialysis (Supplementary Fig. 3b). The protein was confirmed to be PI SVMP by mass spectrometry (Supplementary Fig. 3c). This self-activation of PI SVMP is likely due to residual metal ions in the insect cell media and buffers, trace metal ions leaching off the resin during IMAC purification, and/or a change in pH from the cell culture medium at pH 6 to the purification buffer at pH 8 - the lower pH of the medium being similar to that of the venom gland (pH 5.4), which helps maintain enzyme latency[35]. The PI SVMP zymogen without the C-terminus, including the Avi-tag and His-tag, eluted from the SEC column in one peak at 14.8 ml corresponding to a calculated molecular weight (MW) of ~50 kDa which agrees with the predicted MW for the monomeric zymogen (Fig. 3a). The yield of purified PI SVMP zymogen was 0.63 mg from a 1 L Hi5 insect cell culture.

Following observation of the loss of the SVMP PI C-terminus during purification, a new protein construct was designed with the Avi- and His-tags fused C-terminally to the observed proteolytic degradation site as suggested by MW loss seen by SDS-PAGE and AlphaFold 2 models[33], giving rise to a shorter construct (PIΔC). In fact, this new C-terminus of the MP domain aligns with that of fully characterised PI SVMPs[36-38]. During IMAC affinity purification, the zymogen (predicted MW: 45.4 kDa)

underwent partial activation, resulting in cleavage between the MP (theoretical MW: 26.2 kDa) and prodomain (theoretical MW: 19.3 kDa) (Supplementary Fig. 4a). Subsequent IEX allowed for the isolation of a small amount of MP domain alone, however the bulk of the MP remained bound to the prodomain, forming a stable complex despite cleavage. The MP domain alone eluted from the SEC column at a MW of ~29 kDa, corresponding to the MW expected for the monomeric MP domain (Supplementary Fig. 5a). The metalloproteinase in complex with the prodomain eluted from the SEC column in a different peak corresponding to a MW of ~48 kDa, confirming that the cleaved prodomain and MP domain form a stable assembly with a 1:1 stoichiometry (Supplementary Fig. 5b). The yield of PIΔC was 0.44 mg for the MP domain and 3.25 mg for the MP with non-covalently bound prodomain from a 1 L Hi5 insect cell culture.

The PII SVMP zymogen was purified as intact zymogen and did not undergo any (self-)cleavage throughout purification (Fig. 3b). In SEC, a small amount of protein eluted in the void volume, likely due to the very high concentration of PII zymogen when loaded onto the column, possibly causing some aggregation. The majority of PII SVMP zymogen eluted with a small peak corresponding to ~198 kDa (p2) and a large, sharp peak corresponding to ~84 kDa (p3). SDS-PAGE analysis with non-reducing loading dye suggests that peak p2 corresponds to a PII zymogen dimer (Supplementary Fig. 6a, b). Peak p3 corresponds to the monomeric PII SVMP zymogen, which has a predicted MW of 56 kDa, in agreement with its elution volume in SEC. The yield of PII SVMP zymogen was 8.3 mg (peak 3) from a 1 L Hi5 insect cell culture.

The PIII SVMP zymogen underwent partial activation during the purification process, similar to that of the PI SVMP (PIΔC). This was observed following elution from the IMAC column (Supplementary Fig. 4b) and resulted in the presence of three bands in SDS-PAGE (Fig. 3c), corresponding to the zymogen (predicted MW 70.2 kDa), mature SVMP (MP domain, disintegrin-like domain and cysteine-rich domain) with a predicted MW of 50.6 kDa, and the prodomain with a MW of 19.6 kDa. Interestingly, despite the processing of some PIII molecules, the protein still eluted in one peak from the SEC, at a MW of ~108 kDa based on the elution volume. This indicates that the prodomain again remains associated with the mature SVMP following cleavage,

as previously observed for the PI SVMP (PIΔC) (Supplementary Fig. 4a). The yield of the PIII SVMP was 2.2 mg from a 1 L Hi5 insect cell culture.

We observed a difference in the calculated MW based on SEC elution volume (~108 kDa) and the predicted MW (70 kDa) for the PIII SVMP zymogen. Similarly, the PIII zymogen and mature PIII SVMP both run at a higher-than-expected MW on SDS-PAGE (~80 kDa and ~60 kDa, respectively). This extra size could be attributed to the presence of N-glycans on the mature SVMP. The NetNGlyc 1.0 server predicts 2 glycosylation sites in the mature PIII SVMP[39], and we therefore tested all purified SVMP zymogens for glycosylation using Peptide:N-glycosidase F (PNGase F) (Supplementary Fig. 7). The bands corresponding to PI and PII SVMPs did not change in the presence of PNGase F. However, we observed a downward shift in the MW of the bands corresponding to the PIII zymogen and mature PIII SVMP protein in SDS-PAGE following treatment with PNGase F. De-glycosylation of PIII proteins produced bands at ~77 kDa and ~57 kDa, closer to their predicted MWs. We conclude that the PIII SVMP we produced is highly likely to be glycosylated, and possibly not all of the glycosylation could be removed by PNGase F treatment.

In conclusion, by using the protocol we have developed, we can produce highly purified recombinant SVMP PI, PII and PIII zymogens, each in mg quantities per litre expression culture.

Co-expression of protein disulphide isomerases

Venom gland transcriptomic studies have shown that snake venom glands express several chaperones such as protein disulphide isomerases (PDI), heat shock proteins and calreticulin, alongside venom toxins[40]. These chaperones are expected to be essential for the correct folding of complex, disulphide-rich toxins. In particular, PDIs assist in the formation, breakage and rearrangement of disulphide bonds, stabilizing the proteins. Successful folding of venom peptides aided by PDI was previously demonstrated for marine cone snails[41]. Moreover, overexpression of PDI during recombinant protein expression has also been shown to increase overall protein yield[42]. Therefore, we hypothesised that co-expression of SVMPs with PDI could increase SVMP protein yields due to enhanced disulphide bond formation, enabling more protein to be correctly folded and secreted, potentially reducing protein aggregation. To test our hypothesis, we selected two PDIs, a human PDI

(UniProt: P07237) and a snake PDI (from *Echis ocellatus*)[28], which is overexpressed in venom gland tissue. We generated expression cassettes for human PDI or snake PDI alongside our SVMPs and used Cre-LoxP recombination to integrate these cassettes into our SVMP expression constructs[43].

Successful co-expression of human PDI or snake PDI, alongside our SVMPs, was confirmed by Western Blot and mass spectrometry analysis (Supplementary Fig. 8a). Contrary to our expectation, however, co-expression of PII and PIII SVMP zymogens with these PDIs did not improve the yield of SVMP zymogens: The SEC chromatograms for PII SVMP zymogens after IMAC and IEX purification expressed in the presence and absence of co-expressed PDI aligned perfectly, with identical peak areas (Supplementary Fig. 8b). Similarly, the SEC chromatograms for purified PIII SVMP zymogens are virtually identical in the presence or absence of PDIs (Supplementary Fig. 8c). We conclude that PDI overexpression in insect cells does not enhance the expression and/or folding of SVMP, and therefore did not result in a noticeable improvement in yield.

Activation of SVMPs

Autocleavage of the prodomain in native zymogens is thought to result in the removal of the propeptide from the active site, and therefore activation of the enzyme. SVMP zymogens are theoretically inactive enzymes, maintained in this state by the cysteine switch mechanism of the propeptide within the prodomain (Fig. 2d). Zymogens are activated by an unknown mechanism in venom, removing the propeptide from the active site, rendering it accessible to substrates, with Zn^{2+} as an essential cofactor. We thus hypothesised that activation of our purified zymogens could be achieved by addition of Zn^{2+} ions. We optimised the Zn^{2+} concentration for activation for each SVMP (Fig. 3d-f). Incubation with Zn^{2+} ions was carried out at 37°C for 18 hours.

The PI SVMP zymogen could be close to completely activated by 750 μM $ZnCl_2$ (Fig. 3d). When analysed by SDS-PAGE, the ~45 kDa band corresponding to the zymogen mostly disappears, and two lower MW bands of ~23 kDa and ~26 kDa appear, corresponding to the prodomain and MP domain, respectively. The two proteins could not be separated under the native conditions of SEC, indicating that the prodomain remains stably bound to the MP domain, despite cleavage (as

observed for PIΔC, Supplementary Fig. 5b). Separation of the MP and prodomain has occurred during SDS-PAGE, however, due to the denaturing and thiol-reducing conditions used. AlphaFold 2[29] generated models (Fig. 2d) suggest the prodomain is located on the opposite side of the MP domain, distal from the active site. Thus, bound prodomain is not expected to interfere with the ability of the metalloproteinase to bind and cleave substrates, once the propeptide has been detached from the active site.

The truncated PI SVMP construct (PIΔC) was almost completely cleaved into mature protein during purification, however this protein was not fully active in activity assays (data not shown). For full activity, the PI SVMP (PIΔC) was incubated with 300 μM $ZnCl_2$. Despite complete cleavage of the zymogen, the resulting prodomain and MP domain could not be separated, as was the case for the full-length PI, and, thus, no pure MP was isolated from this construct either (Supplementary Fig. 9). Because this PI (PIΔC) SVMP corresponds better to the venom-derived version of PI SVMP protein, PIΔC was used in all further activity assays and referred to as PI SVMP from here on.

The PII SVMP zymogen was completely activated by 750 μM $ZnCl_2$ (Fig. 3e). Notably, when analysed by SDS-PAGE, a clear separation of prodomain and mature protein was not observed. The band migrating at ~40 kDa corresponds to MP and disintegrin (confirmed by Western blot, Supplementary Fig. 6c). This band disappears with higher concentrations of Zn^{2+} and/or longer incubation times. The band migrating at ~8 kDa is thought to correspond to the processed disintegrin domain but could not be confirmed by Western blot likely due to loss of tags. After incubation for 1 week, only the 8 kDa and 23 kDa bands remained (Fig. 3e). Based on apparent MW, these bands are speculated to correspond to the disintegrin and prodomain, respectively. In summary, PII SVMP has undergone further processing to remove the disintegrin from the MP domain, and the MP domain appears to be unstable over time.

The PIII SVMP zymogen was completely activated by the addition of 600 μM $ZnCl_2$ (Fig. 3f). as evidenced by the disappearance on SDS-PAGE of the ~77 kDa band corresponding to the zymogen. Instead, a band appeared at ~60 kDa corresponding to the mature SVMP (MP domain plus disintegrin-like domain and cysteine-rich

domain) together with a band at ~25 kDa corresponding to the prodomain. Notably, at higher concentrations of Zn^{2+}, the prodomain band appears to have been degraded by the PIII.

We conclude that all SVMP zymogens studied can be activated by incubation with Zn^{2+}, leading to cleavage of the prodomain from the zymogen and, in the case of PII SVMP, further proteolysis into the constituent parts.

Casein and fibrinogen degradation assays

Degradation of casein is a general SVMP activity assay that is used in functional assays for all SVMP classes[26]. SVMP zymogens were supplemented with optimal concentrations of $ZnCl_2$ for SVMP activation (Fig. 3d-f) and incubated with 0.525 µg/µl (~23 µM) casein overnight at 37ºC. The degradation of casein was analysed by SDS-PAGE; indicated concentrations relate to input SVMP zymogen concentrations (Fig. 4a-f). The PI SVMP degraded casein (Fig. 4a); activity was observed when adding 73 nM PI, and complete degradation of casein occurred at the addition of 1.17 µM PI. The PII SVMP exhibited weak activity against casein (Fig. 4b), which may be due to the self-degradation of the MP domain observed during Zn^{2+} activation (Fig. 3e). Casein degradation was observed when adding 1.36 µM PII, as evidenced by the emergence of lower MW bands (Fig. 4b). The PIII SVMP was active against all casein chains (Fig. 4c), with activity seen from concentrations as low as 47 nM PIII, and complete digestion of casein was observed with 343 nM PIII.

Next, we performed fibrinogen degradation assays followed by SDS-PAGE analyses (Fig. 4d-f). None of our recombinant SVMPs had a strong activity against the γ chain of fibrinogen, as is usually the case with SVMPs[38]. However, PI, PII and PIII SVMPs degraded Aα and Bβ chains of fibrinogen to different extents:

The majority of PI SVMP activity is directed against the Aα chain of fibrinogen (Fig. 4d), with the lowest amount of enzyme tested (73 nM). At higher concentrations of PI (585 nM), activity towards the Bβ chain was also observed. Therefore, PI SVMP can be classified as an alpha/beta fibrinogenase, with a preference for the Aα chain. PII SVMP caused removal of fibrinopeptide B (FpB) from the Bβ chain (Fig. 4e) at a concentration of 340 nM. At higher concentrations (680 nM or more), the Aα chain was also degraded. Thus, PII SVMP is an alpha/beta fibrinogenase with a preference for the Bβ chain.

PIII SVMP degraded the Aα chain of fibrinogen at the lowest concentration of PIII tested, 21 nM (Fig. 4f). When supplementing 85 nM PIII or more, the band at 60 kDa corresponding to the Bβ chain disappears as well. Thus, we classify PIII SVMP as an alpha/beta fibrinogenase, with a preference for the Aα chain.

As described above, we also expressed recombinant PII and PIII SVMPs in the presence of co-expressed human or snake PDI, but without an improvement in yield. It remained possible, however, that the activity of these SVMPs could have been enhanced by the co-expression of the PDIs resulting in improved protein folding, e.g. through optimised disulphide bond formation. When tested against fibrinogen, however, the activities of the different SVMPs remained unchanged by PDI co-expression (Supplementary Fig. 8d,e).

To summarise, all recombinant SVMPs (PI, PII, PIII) degraded casein, confirming their activity. They also degraded the alpha and beta chains of fibrinogen in a fibrinogenolytic manner, rather than cleaving fibrinopeptides in a thrombin-like manner.

Fluorogenic peptide and insulin B degradation assays

We next tested if the SVMPs cleave a quenched fluorogenic substrate, ES010 (R & D Systems) which is commonly used to study SVMPs[44] and matrix metalloproteinases[45] for small molecule therapeutic discovery. PIII SVMP was able to cleave the Gly-Leu bond in ES010 (Fig. 4g). In contrast, SVMPs PI and PII did not effectively cleave this substrate under the conditions tested (not shown). Using 20 nM zymogen concentration (corresponding to 90 ng PI, 110 ng PII and 140 ng PIII enzyme concentration/well), the reaction was carried out at 25°C in 50 mM Tris, 300 mM NaCl, pH 7.5 in a 96 well plate and not stirred. The rate of reaction (monitored by fluorescence increase) was plotted against varying substrate concentrations (ranging from 0 μM to 180 μM), and a Michaelis-Menten curve was calculated (Fig. 4g). The low K_M of 19.6 μM indicate a high binding affinity of the PIII SVMP for the ES010 fluorogenic substrate. The high catalytic efficiency (k_{cat}/K_M) of 3.26 x10^7 $M^{-1}s^{-1}$ further suggests that the PIII SVMP is highly effective and specific in processing this substrate. For comparison, a k_{cat}/K_M value of 4,471 $M^{-1}s^{-1}$ was reported for matrix metalloproteinase MMP10 for an ESO10-derived peptide[46], and k_{cat}/K_M values of 30,000 $M^{-1}s^{-1}$ for a triple-helical peptide for MMP-2[47]. Together,

these parameters demonstrate that the recombinant PIII SVMP exhibits both strong substrate affinity and high catalytic efficiency toward a prototypical PIII SVMP substrate.

Next, we assayed the activity of SVMPs PI and PIII against insulin B, a test substrate used previously in SVMP characterisation[16]. Degradation of insulin B at multiple sites was visualised by RP-HPLC. PI and PIII showed distinct insulin B degradation patterns indicating different sequence specificities and cleavage sites. PIII SVMP cleaves insulin B into 6 products (Fig. 4h). PI SVMP cleaves insulin B into 5 products (Fig. 4i). Importantly, this PI SVMP can also be readily purified from *Echis ocellatus* venom. Therefore, we could compare insulin B cleavage by our recombinant PI SVMP with insulin B cleavage by the native source-purified PI enzyme. Identical degradation products of insulin B were observed. Thus, our recombinant PI SVMP is active and has the same substrate specificity as the native enzyme from venom, underscoring that our recombinant expression strategy leads to native-like SVMPs, compellingly validating our approach.

PII and PIII SVMP platelet aggregation assays

Some haemorrhagic SVMPs can disrupt cell adhesion and prevent haemostasis by interfering with platelet aggregation[48]. SVMPs with either a disintegrin (PIIs), or disintegrin-like domain (PIII) can inhibit platelet aggregation through a motif found in these domains. Most commonly, this corresponds to a RGD sequence, which binds integrins. Binding of disintegrin to integrin $\alpha_{IIb}\beta_3$ can be measured through inhibition of ADP-induced platelet aggregation whereby turbidity is determined by flow cytometry (Fig. 5a). Platelet aggregation was close to completely inhibited by the PII SVMP, in both the zymogen and mature, Zn^{2+}-activated enzyme form confirming that the disintegrin is active. Based on our results, the presence of the prodomain in the zymogen has no inhibitory effect on the RGD-containing disintegrin domain, as anticipated. In comparison, the PIII SVMP did not inhibit ADP-induced platelet aggregation (Fig. 5a). Instead of an RGD motif, this PIII SVMP has a divergent ‘RSECD’ motif in its disintegrin-like domain which most likely does not interact with integrin $\alpha_{IIb}\beta_3$. We conclude that our recombinant PII SVMP inhibited platelet aggregation, confirming disintegrin activity in the context of both the zymogen and also the activated PII SVMP.

Thrombin clot time assays

Thrombin clot time assays measure the time required for thrombin to convert fibrinogen to fibrin, leading to clot formation. This assay is used in the clinic to highlight abnormalities in fibrinogen and fibrin clot formation. In our assays, thrombin was replaced with each SVMP to identify the thrombin-like activity of the enzyme. The assay measures turbidity, which is plotted against time. The first and second derivatives are plotted on the same graph, and the maximum rate of change of turbidity (the peak in the 2nd derivative) indicates the time of clot formation. When thrombin is added, fibrin clot formation requires 16.5 seconds (Fig. 5b). As a positive control and example of pro-coagulant SVMPs, thrombin was replaced with native PIII SVMPs purified from *Echis ocellatus* venom. Fibrin clot formation occurs in 28.1 seconds in the presence of *Echis ocellatus* PIII SVMPs (Fig. 5c), confirming clot formation and pro-coagulation activity. However, when replaced with the recombinant PIII SVMP (from *Echis carinatus sochureki*) no clot formation occurs (Fig. 5d). This shows that our recombinantly produced PIII SVMP has no pro-coagulant activity.

MTT cytotoxicity assay

HaCaT cells, immortalized human keratinocyte cells commonly used in dermatological, toxicological, and cancer research, were incubated with PI, PII and PIII SVMPs for 24 hours (100 µg/ml SVMP in standard medium). Cytotoxicity was monitored using the MTT (3-(4,5-dimethylthiazol-2-yl)-2,5-diphenyltetrazolium bromide) assay[49]. The resulting percentage cell viability was calculated as described in the Methods part. At the tested concentration, PII SVMP showed minimal cytotoxicity (Fig. 5e). However, PI and PIII SVMPs were more cytotoxic, with cell viability decreasing by 40% and 50% after 24 hours, respectively (Fig. 5e). The cytotoxic effect of our PIII SVMP (*Echis carinatus)* is comparable to that of crude *Echis carinatus* venom on HEK 293T cells, which induces 63% cytotoxicity with 100 µg/ml venom after 3 hours[50]. Published IC_{50} values for HaCaT cells treated with whole venom for 24 hours fall between 10 and 100 µg/ml[51], however it is important to highlight the distinction between the complex cocktail of toxins found in venom and the homogenous, purified SVMP evaluated in this study.

DISCUSSION

The characterisation of SVMP toxins, critical for effective bioprospecting and the discovery of snakebite therapeutics, is severely hampered by difficulty in isolating the native proteins. To overcome this obstacle, we established here a generic protocol for efficient recombinant production of the three structurally diverse classes of SVMPs. We demonstrated expression of PI, PII and PIII SVMPs from *Echis* species in high quality and quantity using the MultiBac baculovirus/insect cell expression system. SVMP production is challenging given the intricate architecture of SVMPs, notably the many cysteines present in their amino acid sequence with proper folding depending on native disulphide bond formation. Moreover, the severe cytotoxicity of these enzymes leads to premature cell death when expressed in their mature SVMP form. Various initial strategies we tried, involving production of active site SVMP mutants and expression in the presence of a small molecule SVMP inhibitor (classical approaches for enzyme production), did not alleviate the adverse cytotoxic effects of the SVMPs in the insect cells used as a production host. Although protein expression was achieved in all cases, our results showed that these strategies are not viable routes to produce high yields of active SVMPs. We hypothesized that co-expression of SVMPs with human or snake PDI would aid their proper folding, ensuring the multiple disulphide bonds were correctly formed and thus improving yields and/or activity of the SVMPs. However, co-expression of either a snake PDI, or a commonly used human PDI, neither improved protein yields nor enzyme activity. We conclude that the endogenous insect cell PDIs are sufficient for SVMP folding in our setup. Alternatively, a combination of different chaperones may be required for further boosting SVMP production.

The addition of the N-terminally fused prodomain unlocked the production of the SVMPs. The toxin is generally maintained in an inactive state by the highly conserved propeptide sequence which blocks the active site of the MP domain. This propeptide is clamped in place by the N-terminal prodomain. Despite expression as a zymogen, residual cytotoxicity was still observed, evident by the decrease in cell viability throughout expression and reduction in the amount of co-expressed YFP fluorescence due to cell lysis (Fig. 2). In agreement with this observation, PI and PIII SVMPs were able to partially activate themselves, resulting in the presence of three characteristic bands in Coomassie-stained SDS-PAGE – the zymogen, mature

SVMP and prodomain. We speculate that this self-cleavage could be due to the SVMP active site accreting divalent metal ions from the media and buffers used. Additionally, it is likely that the change in pH from 6 (expression) to pH 8 (purification) allows the activation of SVMPs, as is the case when venom is released from the venom gland (pH 5.4) into the victim during envenoming[35].

Of note, despite the self-cleavage of the PI and PIII zymogens, the majority of the mature SVMP protein in both cases remained associated with the prodomain. Interestingly, this did not affect the activity of the SVMPs. According to AlphaFold 2 structure predictions, the prodomain is located on the side of the MP domain which is opposite from the active site. Upon activation, cleavage of the prodomain releases the propeptide from the active site. This renders the active site Zn^{2+} free to interact with a substate. We observe that the SVMPs are active even if the prodomain, now no longer covalently linked to the SVMP, remains bound to the MP domain (Fig. 3c, Supplementary Fig, 4).

Alongside the processing into the mature protein, the SVMP zymogens also undergo further post-translational processing. The PI SVMP construct described here was based on transcriptomic data and corresponds to the Uniprot sequence Q2UXQ3. During purification, it underwent C-terminal truncation by approximately 10 kDa, leading to a smaller protein which corresponds closely to previously characterised PI SVMPs[36-38]. Additionally, we observed a general trend of C-terminal tandem oligohistidine- and avi-tag loss during purification, activation and subsequent activity assays in the case of all three SVMPs.

SVMPs from all three classes were activated by the addition of Zn^{2+} ions. While some PI SVMP was processed during purification, any remaining PI zymogen could be cleaved into the mature SVMP and prodomain by incubation with Zn^{2+}. The PII zymogen could be activated by the same means, although there was no clear separation into prodomain and mature protein. Instead, we observed two bands corresponding to the disintegrin and prodomain after prolonged incubation with Zn^{2+} (Fig. 3e). It is unlikely that the observed disappearance of the MP domain is due to misfolding because the PII zymogen is well expressed with high yields (9-10 mg/L culture) in insect cells and eluted in two clean peaks in SEC corresponding to a monomer and dimer, respectively. In the case of misfolding, we would have expected aggregation and/or degradation during purification, and we would not expect to see

degradation of the zymogen in SDS-PAGE analysis only after addition of Zn^{2+} which activates the metalloproteinase (Fig. 3e). Notably, the disintegrin domain of this PII has 100% sequence identity to ocellatusin, a short, monomeric disintegrin and major component of *Echis ocellatus* venom[52]. Previous studies have identified a discrepancy between the amounts of ocellatusin and its PII SVMP precursor in the venom, whereby ocellatusin represents 3.9%, and the PII SVMP less than 0.1% of venom proteins[5]. Taken together, these findings suggest that the disintegrin is likely liberated from this PII SVMP, and is the more pathogenic component of the SVMP, causing inhibition of platelet aggregation (Fig. 5a). In contrast, the metalloproteinase domain is unstable and therefore requires high toxin concentrations to elicit proteolytic activity in our activity assays (Fig. 4b, 4e).

The recombinant PIII zymogen was fully activated in our experiments by the addition of Zn^{2+} ions (Fig. 3f). Interestingly, this PIII SVMP was able to degrade the prodomain despite the latter initially remaining bound to the mature protein according to SEC (Fig. 3c). This agrees with the finding that prodomains are rarely identified in the venom proteome[53], suggesting that prodomains might eventually be fully degraded by venom proteases.

Once activated, all recombinant SVMPs were active against bovine casein, a general protease substrate (Fig. 4a-c). PI and PIII exhibited strong activity, degrading all bands, while PII was significantly less active in line with the observed MP domain degradation discussed above.

The fibrinogen degradation assay is particularly relevant for SVMPs and indicates their potential haemotoxic activity (Fig. 4d-f). The 340 kDa fibrinogen glycoprotein is made up of three pairs of polypeptide chains, which lead to three groups of distinct bands when analysed by reducing SDS-PAGE: the Aα (70-75 kDa), Bβ (65 kDa) and γ (50 kDa) chains. In contrast to the endogenous serine protease thrombin, which cleaves fibrinopeptides A and B off the Aα and Bβ chains, causing self-polymerisation into fibrin fibres and formation of blood clots[54], the PI, PII, and PIII SVMP studied here caused a fuller degradation of fibrinogen (Fig. 4 d-f). All SVMPs were active against both the Aα and Bβ chains of fibrinogen; the PI and PIII showed a preference for the Aα chain and the PII preferentially degraded the Bβ chain of fibrinogen. In agreement, no fibrin clot formation was observed for our recombinant PIII SVMP during thrombin clot time assays (Fig. 5d). We conclude that the three

SVMPs interfere with clot formation and would thus contribute to an anticoagulant outcome upon envenoming. The PIII SVMP cannot cause clot formation in the thrombin clot time assay (Fig. 5d), suggesting it is not an ecarin-like prothrombin activator, which is typically responsible for procoagulant activity seen in such assays with *Echis* venoms (Fig. 5c).

As observed for casein degradation, PII SVMP is less active than PI and PIII SVMPs, requiring much higher enzyme concentrations to observe fibrinogen cleavage. This agrees with our previous observation that bands corresponding to the MP-disintegrin protein or the MP domain alone after activation with Zn^{2+} (Fig. 3e) are absent in SDS-PAGE, indicating that the MP domain is likely unstable.

Moreover, the recombinant SVMP PIII was highly active against a fluorogenic peptide substrate, ES010, showing high affinity and specificity for cleavage of the Gly-Leu bond within the peptide (Fig. 4g). In this context, we would like to point out that enzyme concentrations and kinetics are based on zymogen concentrations, assuming 100% SVMP activation by Zn^{2+} (Fig. 4a-g). If zymogen activations were incomplete or non-linear, our k_{cat}/K_M calculation presents an underestimate of the PIII SVMP's catalytic efficiency (Fig. 4g).

The SVMP PIII was also active against insulin B (Fig. 4h), as was SVMP PIΔC (Fig. 4i) which produced identical degradation products to native PI, confirming identical cleavage sites and successful recombinant production of toxin with native-like characteristics, validating our approach.

In addition to the proteolytic activity of the MP domain, PII and PIII SVMPs also include a disintegrin or disintegrin-like domain containing a potential integrin binding motif. In platelet aggregation assays, our RGD-containing PII SVMP inhibited ADP-induced platelet-aggregation with and without the prodomain present (Fig. 5a). The RSECD-containing PIII, in contrast, did not inhibit ADP-induced platelet aggregation, but this does not exclude disintegrin-like activity of this domain.

SVMPs are structurally and functionally related to ADAMs (A Disintegrin and Metalloproteinases) and MMPs (Matrix Metalloproteinases), which are involved in cell-cell interactions, ectodomain shedding and degradation of extracellular matrix components respectively[55]. For MMPs, zymogen expression in mammalian and insect cells has been reported and enzyme activation was achieved via 4-

aminophenylmercuric acetate or trypsin to remove the prodomain[56,57]. Similarly, ADAMs have been expressed with their prodomain in mammalian and insect cells to aid proper folding and latency[58,59]. The ADAMs prodomain has been removed post-translationally, e.g. by co-expression of furin[60]. Interestingly, in agreement with our PI and PIII SVMP observations, ADAM33 zymogen was processed and secreted in *Drosophila S2* cells, with the prodomain remaining associated with the catalytic domain after purification. The processing was enhanced by addition of cadmium chloride and zinc chloride[61]. Due to their critical involvement in pathological processes such as cancer, inflammation and fibrosis, ADAMs and MMPs have become prominent targets in drug discovery[62,63]. While ADAMs and MMPs are well characterised in the literature, comparable insights into SVMPs are largely absent to date, due to lack of means for recombinant SVMP protein production.

Here, we present a novel, potent and efficient platform for the recombinant production of all three classes of SVMPs as zymogens, overcoming their high cytotoxicity. We anticipate that our protocol will unlock the production of many additional hitherto unaccesible SVMPs, allowing in-depth characterisation of their post-translational processing, enzymatic activity, substrate specificity, cyto- and haemotoxicity, and enable the evaluation of potential biomedical applications to develop new diagnostics and treatments for blood clotting disorders. Our recombinant production approach also paves the way to engineer existing and new SVMPs for improved and novel applications in haematology, thrombosis and inflammation research and other important areas in which SVMPs can play a crucial role. Importantly, the recombinantly produced, tagged SVMPs can serve as antigens for the future selection and evolution of neutralising antibodies as a basis for next-generation snakebite treatment to combat SBE.

METHODS

SVMP expression construct design

PI, PII and PIII SVMP constructs were designed by fusing an Avi- and His-tag (GGSGLNDIFEAQKIEWHEHHHHHHHH*) to the C terminus of the native SVMP sequences listed on UniProt (PI - Q2UXQ3, PII - A0A3G1E3U2, PIII - E9JG34). The sequences were codon-optimised for *Spodoptera frugiperda*, gene synthesised (Genscript) and inserted into the plasmid pACEBac1, which acted as the donor in the MultiBac system[64]. Structure predictions of SVMP zymogens were performed using AlphaFold 3[34] in the presence of a single Zn^{2+}. Per residue predicted Local Distance Difference Test (pLDDT) plots, indicating local confidence, were generated from B-factor values stored in the .cif files. The highest-ranked model among the five predictions was selected for visualization and figure generation using ChimeraX.

Mature SVMP constructs did not include the prodomain, but did contain an N-terminally fused melittin signal sequence (MKFLVNVALVFMVVYISYIYA). Propeptide-SVMP fusions contained an additional N-terminally fused propeptide triplicate and TEV site (GGSPKMCGVTPKMCGVTPKMCGVTENLYFQSN) following the melittin signal sequence. SVMP active site mutants were based on the mature SVMP constructs, but with the active site glutamic acid mutated to aspartic acid and glycine mutated to cysteine[31]. Zymogen constructs comprised the native signal sequence preceding the native prodomain (which is specific to the SVMP) and the SVMP sequence with a C-terminal Avi-His-tag fusion. PI was found to undergo C terminal processing, the site of which was predicted by modelling using AlphaFold 2[33]. PIΔC construct contained the Avi-His-tag fusion following this site.

Recombinant SVMP expression

Each SVMP-containing pACEBac1 plasmid was expressed using the MultiBac baculovirus/insect cell expression following established protocols[65]. SVMPs were expressed in Hi5 insect cells at 19°C, in ESF 921 Insect Cell Culture Media (Expression Systems). The cells were monitored throughout expression by measuring YFP fluorescence (encoded in baculoviral genome) and cell viability (by determining percentage of alive cells using Trypan Blue). A control expression of an unrelated, non-toxic protein (E3 ligase) was used as a control for YFP and cell viability measurements. Expression in the presence of Marimastat was tested using

a final concentration of 0 μM, 3 μM and 6 μM Marimastat in the cell culture media, which was added alongside the virus (at the start of expression). Cultures were harvested 5 days after infection by centrifugation (1000 xg, 10 minutes), or when the cell viability was 0% if this occurred sooner. The secreted SVMP proteins were purified immediately after harvesting from the supernatant.

Co-expression of SVMPs with protein disulphide isomerase

The PII and PIII SVMPs were additionally co-expressed with human or snake protein disulphide isomerase (PDI) which was incorporated into the plasmid using Cre-lox[43]. The multigene expression construct was made using PDI-containing pIDC plasmids as the donor plasmid and SVMP-containing pACEBac1 plasmids as the acceptor plasmid. SVMP expression was carried out as above.

Recombinant SVMP purification

Clarified media (containing SVMP) was continuously passed through HiTrap IMAC FF 5 ml column (Cytiva) at 2 ml/min, for 18 hours at 4°C using a peristaltic pump. Subsequently, the column was washed with 10 CV High Salt Buffer (50 mM Tris-Cl, 1 M NaCl, pH 8.0) and 10 CV SVMP Buffer (50 mM Tris-Cl, 300 mM NaCl, pH 8.0). After the washing steps, the IMAC column was attached to an AKTA Pure system. The SVMP was eluted from the IMAC column using a gradient of imidazole from 0 mM to 500 mM imidazole in SVMP buffer. Fractions containing SVMP were pooled and dialysed into SVMP Low Salt Buffer (50 mM Tris-Cl, 50 mM NaCl, pH 8.0). SVMP was further purified by ion exchange chromatography by passing the dialysed protein through a 5 ml HiTrap Q XL column. Subsequently, the SVMP was eluted from the column by a gradient of 50 mM to 1 M NaCl in SVMP buffer. Fractions containing SVMP were pooled and concentrated to 500 μl (maximum 10 mg/ml). Finally, SVMP was purified by size exclusion chromatography (SEC) using an Superdex 200 increase 10/300 GL column (Cytiva) in SVMP buffer with a flow rate of 0.375 ml/min. Cytiva Gel Filtration Calibration Kits were used to calibrate the column, with elution peaks plotted to generate a standard curve with which to calculate the molecular weights (MWs) of SVMP proteins. Eluted SVMP was concentrated to 0.5 - 2 mg/ml using an Amicon concentrator with appropriate MW cut off. Glycerol was added to 5% before the protein was flash frozen in liquid nitrogen and stored at -80°C.

Purification of PIII SVMP fraction of *Echis ocellatus* venom

As a procoagulant control for blood clot time assays, an *Echis ocellatus* SVMP PIII fraction was prepared using SEC. Whole venom (25 mg) was dissolved in 1.5 ml of PBS (25 mM sodium phosphate, 0.15 M NaCl, pH 7.2), centrifuged and the supernatant loaded onto a 120 ml column of Superdex75 (Cytiva). Proteins were separated in PBS using a flowrate of 1.0 ml/min and the separation was monitored at 280 nm. Two ml fractions were collected, and SDS-PAGE was used to determine the fractions containing SVMP PIIIs. These were pooled and shown to be free of serine protease activity using the casein degradation assay (see below) with appropriate inhibitors.

SVMP deglycosylation assay

Glycosylation of SVMP zymogens was determined by incubation with peptide-*N*-glycosidase F (PNGase F, Promega) to remove N-linked oligosaccharide groups, followed by SDS-PAGE. Briefly, the reaction was carried out with 1-2 µg SVMP diluted in 12 µl water, followed by addition of 1 µl 5% SDS and 1 µl 1 M DTT. Next, the sample was heated at 95°C for 5 minutes to denature the SVMP zymogens. Once cooled at room temperature, 2 µl SVMP Buffer, 2 µl 10% NP-40 and 2 µl PNGase F were added. The reaction mix was incubated at 37°C for 3 hours. Subsequently, SDS-PAGE sample buffer (reducing) was added, and the samples were analysed by SDS-PAGE. SVMP zymogen deglycosylation was identified by a shift towards lower MW of the SVMP band compared to the band where PNGase F was omitted.

SVMP enzyme activation

To determine optimal activation conditions, SVMP was titrated with 0 – 750 µM $ZnCl_2$, then incubated at 26°C or 37°C for 18 hours. Activation was monitored using SDS-PAGE and disappearance of the SVMP zymogen band in Coomassie-stained gels.

Casein and fibrinogen degradation assays

Activated SVMP was titrated into a freshly prepared 20 µl reaction mix containing casein or fibrinogen at a final concentration of 0.525 mg/ml in SVMP Buffer. Final SVMP concentrations ranged from 0 to 2.34 µM (based on SVMP zymogen concentration at the start of the experiment). The negative control contained 5 mM EDTA as an SVMP inhibitor and maximum concentrations of SVMP (PI - 2.34 µM,

PII -1.07 and 1.34 µM, PIII - 685 nM). Incubation was carried out at 37ºC for 18 hours. SDS-PAGE sample buffer was added, and the samples were heated to 95ºC to stop the reaction, and the degradation pattern was analysed by reducing SDS-PAGE.

Fluorogenic peptide substrate cleavage assay

The quenched fluorogenic peptide Mca-KPLGL-Dpa-AR-NH_2 (ES010, R&D systems Inc.) was used to kinetically measure SVMP activity, whereby the activated SVMP cleaves the Gly-Leu bond. Cleavage leads to release of the Dpa-containing quencher from the fluorescent Mca-containing fragment. ES010 substrate was diluted in reaction buffer (50 mM Tris-Cl, 300 mM NaCl, pH 7.5) and used in the assay at final concentrations of 0 µM to 180 µM, in 100 µl in a 96 well plate. Enzymes were activated with Zn^{2+} (see above) and diluted in reaction buffer before adding 90 ng PI (45 kDa), 112 ng PII (56 kDa) and 144 ng PIII (72 kDa) enzyme to each well, resulting in a final concentration of 20 nM based on the SVMP zymogen concentration at the start of the experiment). Fluorescence was followed for 1 hour at 25ºC using a BioTech Synergy Neo2 instrument, an excitation wavelength of 320 nm and emission wavelength of 405 nm. Measurements were taken in triplicate. Data was plotted using Origin, and a non-linear curve fitted using the Michaelis-Menten function. Origin provided the best-fit values for V_{max} and K_M, and k_{cat} could be calculated by V_{max}/enzyme concentration.

Insulin B degradation assay

Insulin B degradation was determined following the established protocol [16], using a final concentration of 0.02 mg/ml insulin B and 0.01 mg/ml activated SVMP, in in 50 mM Tris-Cl, 150 mM NaCl, 1 mM Ca_2Cl pH 7.5 (TBS) buffer. Incubation was carried out at 37ºC for 120 minutes, then trifluoracetic acid was added to 1% to stop the reaction. The whole sample (= 1 µg insulin B) was analysed by RP-HPLC using a C18 reverse phase column.

Inhibition of ADP-induced platelet aggregation by the PII and PIII SVMPs

The assay was based on the Platelet Activation protocol (BD Biosciences). The following modifications were introduced to the original protocol: Human platelet rich plasma (PRP) was prepared by centrifugation of fresh whole blood from healthy donors at 220 xg for 20 minutes. For each reaction, 10 µl activated SVMP (300 nM

final concentration) was added to 70 µl PRP, 5 µl ADP (20 µM final concentration) and 15 µl FITC Mouse Anti-Human PAC-1 antibody (BD Biosciences). Modified Tyrode's Buffer (134 nM NaCl, 2.9 mM KCl, 0.34 nM $Na_2HPO_4.12H_2O$, 12 mM $NaHCO_3$, 20 mM HEPES, 1 mM $MgCl_2$, 5 mM glucose) was used instead of SVMP for a positive control (ADP only). The reaction was incubated for 30 minutes in the dark at 25°C, prior to fluorescence data acquisition (10,000 events) in a BD Accuri C6 Plus flow cytometer (excitation – 488 nm). Platelet activation data was normalised accounting for the mean FITC fluorescence of the positive control as 100%, and the mean FITC fluorescence of the negative control (no ADP added to the reaction) as 0%. Experiments were performed in triplicate.

Thrombin / SVMP clot time assay

Experiments were carried out following manufacturer's kit instructions (HemosIL, Thrombin Time 0009758515), using an ACL TOP coagulation analyser using 3.0 U/ml thrombin, 500 ng PIII SVMP pool purified from *Echis ocellatus* venom and 500 ng activated recombinant PIII SVMP. The assay measures the rate of increase in turbidity as the fibrin clot forms. The peak in the rate of change (2nd derivative) is considered to be the point of clot formation.

MTT cell viability assay

MTT assay was based on the methods of Hall *et al.*[51]. Immortalized human epidermal keratinocytes, HaCaT, (Caltag Medsystems) were seeded (5,000 cells/well, clear-sided 96-well plates) in standard medium (DMEM high glucose with GlutaMAX^{TM} supplemented with 2 mM sodium pyruvate, 100 IU/ml penicillin, 250 µg/ml streptomycin, 10% Fetal Bovine Serum, 1% GlutaMAX^{TM} (Gibco)), then left to adhere overnight at 37°C, 5% CO_2. The next day, the SVMPs treatments (100 µg/ml) were prepared in standard medium, and cells were treated with each prepared solution (100 µl/well, duplicate wells) for 24 hours. For this assay, the MTT Cell Viability Assay Kit (Biotium) was used: 10 µl of MTT solution was added to the 100 µl of medium in each well and mixed by tapping gently on the side of the tray. The cells were incubated at 37 °C for 4 hours. 200 µl DMSO was added directly into the medium in each well and pipetted up and down several times to dissolve the formazan salt. The absorbance was measured on BioTek Synergy Neo2 spectrophotometer at 570 nm. The background absorbance was also measured at

630 nm (subtracted background absorbance from signal absorbance to obtain normalized absorbance values). The % of cell viability for each treatment well was calculated as follows:

$$\frac{Normalised\ abs\ treatment\ well\ - Average\ normalised\ abs\ blank\ wells}{Average\ normalised\ abs\ cell\ control\ wells - Average\ normalised\ abs\ blank\ wells}$$

IC50s were calculated from the log10 concentration versus normalized response curves using the 'log(inhibitor) vs. normalized response – variable slope' in GraphPad Prism, which uses the following equation:

$$y = \frac{100}{1+10^{[(LogIC50-x)HillSlope]}}$$

where *y* is the normalized % cell viability values and *x* is the $\log_{10}$ of the SVMPs concentrations.

Data availability

Source data are provided with this paper.

ACKNOWLEDGEMENTS

This work was supported by a Horizon 2020 European Innovation Council (EIC) FET OPEN grant 'ADDovenom' (contract nr.899670) to C.S., I.B., R.V, and N.R.C. C.S, I.B. and N.R.C also acknowledge financial support by the Wellcome Trust (221708/Z/20/Z). C.S. and N.R.C. are funded by a UKRI Engineering Biology Mission Award (BB/Y007581/1). K.H. is supported by an EC Marie Sklodowska-Curie Fellowship (101149867; EP/Z002613/1). I.A.C. is funded by a studentship from the BBSRC SWBio Doctoral Training Programme.

AUTHOR CONTRIBUTIONS

C.S., I.B. and N.R.C conceptualized the project. S.H. and I.B. designed expression constructs; S.L. carried out protein structure predictions and assisted in expression construct design. S.H., B.R., K.K.H. and G.B. expressed and purified proteins. R.V. performed SVMP expression tests. D.S. assisted with cloning and protein expression. J.B.F. assisted with casein and fibrinogen degradation and clotting assays. I.A.C. performed platelet aggregation assays, M.C.W. performed insulin B degradation assays and purified native SVMPs, R.S assisted with ES010 assays. M.M.C and A.M. performed blood coagulation assays. All authors were a part of the writing process and final review of the manuscript.

SUPPLEMENTARY INFORMATION

The Supplementary Information contains 9 additional Supplementary Figures.

REFERENCES:

1. Gutierrez, J.M. et al. Snakebite envenoming. *Nat. Rev. Dis. Primers* **3**, 17079 (2017).
2. Longbottom, J. et al. Vulnerability to snakebite envenoming: a global mapping of hotspots. *Lancet* **392**, 673-684 (2018).
3. Oliveira, A.L. et al. The chemistry of snake venom and its medicinal potential. *Nat. Rev. Chem.* **6**, 451-469 (2022).
4. Bittenbinder, M.A. et al. Tissue damaging toxins in snake venoms: mechanisms of action, pathophysiology and treatment strategies. *Commun. Biol.* **7**, 358 (2024).
5. Wagstaff, S.C., Sanz, L., Juarez, P., Harrison, R.A. & Calvete, J.J. Combined snake venomics and venom gland transcriptomic analysis of the ocellated carpet viper, *Echis ocellatus*. *J. Proteomics* **71**, 609-623 (2009).
6. Casewell, N.R. et al. Medically important differences in snake venom composition are dictated by distinct postgenomic mechanisms. *Proc. Natl. Acad. Sci. U.S.A.* **111**, 9205-9210 (2014).
7. Tasoulis, T. & Isbister, G.K. A current perspective on snake venom composition and constituent protein families. *Arch. Toxicol.* **97**, 133-153 (2023).
8. Asega, A.F. et al. Cleavage of proteoglycans, plasma proteins and the platelet-derived growth factor receptor in the hemorrhagic process induced by snake venom metalloproteinases. *Sci. Rep.* **10**, 12912 (2020).
9. Kini, R.M. & Koh, C.Y. Metalloproteases Affecting Blood Coagulation, Fibrinolysis and Platelet Aggregation from Snake Venoms: Definition and Nomenclature of Interaction Sites. *Toxins (Basel)* **8** (2016).
10. Gutierrez, J.M., Rucavado, A., Escalante, T. & Diaz, C. Hemorrhage induced by snake venom metalloproteinases: biochemical and biophysical mechanisms involved in microvessel damage. *Toxicon* **45**, 997-1011 (2005).
11. Gutierrez, J.M., Escalante, T., Rucavado, A., Herrera, C. & Fox, J.W. A Comprehensive View of the Structural and Functional Alterations of Extracellular Matrix by Snake Venom Metalloproteinases (SVMPs): Novel Perspectives on the Pathophysiology of Envenoming. *Toxins (Basel)* **8** (2016).
12. Almeida, G.O., de Oliveira, I.S., Arantes, E.C. & Sampaio, S.V. Snake venom disintegrins update: insights about new findings. *J. Venom Anim. Toxins Incl. Trop. Dis.* **29**, e20230039 (2023).
13. Clissa, P.B., Della-Casa, M.S., Zychar, B.C. & Sanabani, S.S. The Role of Snake Venom Disintegrins in Angiogenesis. *Toxins (Basel)* **16** (2024).
14. Moore, G.W. Snake Venoms in Diagnostic Hemostasis and Thrombosis. *Semin. Thromb. Hemost.* **48**, 145-160 (2022).
15. Slagboom, J., Kool, J., Harrison, R.A. & Casewell, N.R. Haemotoxic snake venoms: their functional activity, impact on snakebite victims and pharmaceutical promise. *Br. J. Haematol.* **177**, 947-959 (2017).

16. Wilkinson, M.C. et al. Complex compositional and functional diversity of venom metalloproteinases in African puff adders. *bioRxiv*, 2024.05.31.596867 (2025).

17. Yee, K.T., Pitts, M., Tongyoo, P., Rojnuckarin, P. & Wilkinson, M.C. Snake Venom Metalloproteinases and Their Peptide Inhibitors from Myanmar Russell's Viper Venom. *Toxins (Basel)* **9** (2016).

18. Olaoba, O.T., Karina Dos Santos, P., Selistre-de-Araujo, H.S. & Ferreira de Souza, D.H. Snake Venom Metalloproteinases (SVMPs): A structure-function update. *Toxicon X* **7**, 100052 (2020).

19. Pinyachat, A., Rojnuckarin, P., Muanpasitporn, C., Singhamatr, P. & Nuchprayoon, S. Albocollagenase, a novel recombinant P-III snake venom metalloproteinase from green pit viper (*Cryptelytrops albolabris*), digests collagen and inhibits platelet aggregation. *Toxicon* **57**, 772-780 (2011).

20. Assakura, M.T., Silva, C.A., Mentele, R., Camargo, A.C. & Serrano, S.M. Molecular cloning and expression of structural domains of bothropasin, a P-III metalloproteinase from the venom of *Bothrops jararaca*. *Toxicon* **41**, 217-227 (2003).

21. Jonebring, A. et al. Expression and characterization of recombinant ecarin. *Protein J.* **31**, 353-358 (2012).

22. Shimokawa, K., Jia, L.G., Wang, X.M. & Fox, J.W. Expression, activation, and processing of the recombinant snake venom metalloproteinase, pro-atrolysin E. *Arch. Biochem. Biophys.* **335**, 283-294 (1996).

23. Camacho, E., Escalante, T., Remans, K., Gutierrez, J.M. & Rucavado, A. Site mutation of residues in a loop surrounding the active site of a PI snake venom metalloproteinase abrogates its hemorrhagic activity. *Biochem. Biophys. Res. Commun.* **512**, 859-863 (2019).

24. Bieniossek, C., Imasaki, T., Takagi, Y. & Berger, I. MultiBac: expanding the research toolbox for multiprotein complexes. *Trends Biochem. Sci.* **37**, 49-57 (2012).

25. Villaflores, O.B. et al. Easy expression of the C-terminal heavy chain domain of botulinum neurotoxin serotype A as a vaccine candidate using a bi-cistronic baculovirus system. *J. Virol. Methods* **189**, 58-64 (2013).

26. Macêdo, J.K.A. & Fox, J.W. Biological Activities and Assays of the Snake Venom Metalloproteinases (SVMPs). In *Venom Genomics and Proteomics. Toxinology.* (ed. Gopalakrishnakone, P., Calvete, J.) (Springer, 2016).

27. Alsolaiss, J., Alomran, N., Hawkins, L. & Casewell, N.R. Commercial Antivenoms Exert Broad Paraspecific Immunological Binding and *In Vitro* Inhibition of Medically Important *Bothrops* Pit Viper Venoms. *Toxins (Basel)* **15** (2022).

28. Redureau, D. et al. Dual Proteomics Strategies to Dissect and Quantify the Components of Nine Medically Important African Snake Venoms. *Toxins (Basel)* **17** (2025).

29. Tessier, D.C., Thomas, D.Y., Khouri, H.E., Laliberte, F. & Vernet, T. Enhanced secretion from insect cells of a foreign protein fused to the honeybee melittin signal peptide. *Gene* **98**, 177-183 (1991).

30. Xie, C. et al. Neutralising effects of small molecule toxin inhibitors on nanofractionated coagulopathic Crotalinae snake venoms. *Acta Pharm. Sin. B* **10**, 1835-1845 (2020).

31. Camacho, E. et al. Novel Catalytically-Inactive PII Metalloproteinases from a Viperid Snake Venom with Substitutions in the Canonical Zinc-Binding Motif. *Toxins (Basel)* **8** (2016).

32. Grams, F., Huber, R., Kress, L.F., Moroder, L. & Bode, W. Activation of snake venom metalloproteinases by a cysteine switch-like mechanism. *FEBS Lett.* **335**, 76-80 (1993).

33. Jumper, J. et al. Highly accurate protein structure prediction with AlphaFold. *Nature* **596**, 583-589 (2021).

34. Abramson, J. et al. Accurate structure prediction of biomolecular interactions with AlphaFold 3. *Nature* **630**, 493-500 (2024).

35. Mackessy, S.P. & Baxter, L.M. Bioweapons synthesis and storage: The venom gland of front-fanged snakes. *Zoologischer Anzeiger* **245**, 147-159 (2006).

36. Sanchez, E.F. et al. The novel metalloproteinase atroxlysin-I from Peruvian *Bothrops atrox* (Jergon) snake venom acts both on blood vessel ECM and platelets. *Arch. Biochem. Biophys.* **496**, 9-20 (2010).

37. Bello, C.A. et al. Isolation and biochemical characterization of a fibrinolytic proteinase from *Bothrops leucurus* (white-tailed jararaca) snake venom. *Biochimie* **88**, 189-200 (2006).

38. Bernardes, C.P. et al. Isolation and structural characterization of a new fibrin(ogen)olytic metalloproteinase from *Bothrops moojeni* snake venom. *Toxicon* **51**, 574-584 (2008).

39. Gupta, R. & Brunak, S. Prediction of glycosylation across the human proteome and the correlation to protein function. *Pac. Symp. Biocomput.*, 310-322 (2002).

40. Junqueira-de-Azevedo, I.L. et al. Venom-related transcripts from *Bothrops jararaca* tissues provide novel molecular insights into the production and evolution of snake venom. *Mol. Biol. Evol.* **32**, 754-766 (2015).

41. Safavi-Hemami, H. et al. Rapid expansion of the protein disulfide isomerase gene family facilitates the folding of venom peptides. *Proc. Natl. Acad. Sci. U.S.A.* **113**, 3227-3232 (2016).

42. Hsu, T.A., Watson, S., Eiden, J.J. & Betenbaugh, M.J. Rescue of immunoglobulins from insolubility is facilitated by PDI in the baculovirus expression system. *Protein Expr. Purif.* **7**, 281-288 (1996).

43. Haffke, M., Viola, C., Nie, Y. & Berger, I. Tandem recombineering by SLIC cloning and Cre-LoxP fusion to generate multigene expression constructs for protein complex research. *Methods Mol. Biol.* **1073**, 131-140 (2013).

44. Nguyen, G.T.T. et al. High-throughput proteomics and *in vitro* functional characterization of the 26 medically most important elapids and vipers from sub-Saharan Africa. *Gigascience* **11** (2022).

45. Azevedo, A., Prado, A.F., Issa, J.P. & Gerlach, R.F. Matrix metalloproteinase 2 fused to GFP, expressed in *E. coli*, successfully tracked MMP-2 distribution *in vivo*. *Int. J. Biol. Macromol.* **89**, 737-745 (2016).

46. Schlage, P., Kockmann, T., Sabino, F., Kizhakkedathu, J.N. & Auf dem Keller, U. Matrix Metalloproteinase 10 Degradomics in Keratinocytes and Epidermal Tissue Identifies Bioactive Substrates With Pleiotropic Functions. *Mol. Cell. Proteomics* **14**, 3234-3246 (2015).

47. Akers, W.J. et al. Detection of MMP-2 and MMP-9 activity *in vivo* with a triple-helical peptide optical probe. *Bioconjug. Chem.* **23**, 656-663 (2012).

48. Takeda, S., Takeya, H. & Iwanaga, S. Snake venom metalloproteinases: structure, function and relevance to the mammalian ADAM/ADAMTS family proteins. *Biochim. Biophys. Acta* **1824**, 164-176 (2012).

49. Mosmann, T. Rapid colorimetric assay for cellular growth and survival: application to proliferation and cytotoxicity assays. *J. Immunol. Methods* **65**, 55-63 (1983).

50. Pierce, R.D. et al. Characterization of crude *Echis carinatus* venom-induced cytotoxicity in HEK 293T cells. *J. Venom Res.* **2**, 59-67 (2011).

51. Hall, S.R. et al. Repurposed drugs and their combinations prevent morbidity-inducing dermonecrosis caused by diverse cytotoxic snake venoms. *Nat. Commun.* **14**, 7812 (2023).

52. Smith, J.B. et al. Characterization of a monomeric disintegrin, ocellatusin, present in the venom of the Nigerian carpet viper, *Echis ocellatus*. *FEBS Lett.* **512**, 111-115 (2002).

53. Moura-da-Silva, A.M. et al. Processing of Snake Venom Metalloproteinases: Generation of Toxin Diversity and Enzyme Inactivation. *Toxins (Basel)* **8** (2016).

54. Weisel, J.W. & Litvinov, R.I. Fibrin Formation, Structure and Properties. *Subcell. Biochem.* **82**, 405-456 (2017).

55. Takeda, S. ADAM and ADAMTS Family Proteins and Snake Venom Metalloproteinases: A Structural Overview. *Toxins (Basel)* **8** (2016).

56. Ogata, Y., Itoh, Y. & Nagase, H. Steps involved in activation of the pro-matrix metalloproteinase 9 (progelatinase B)-tissue inhibitor of metalloproteinases-1 complex by 4-aminophenylmercuric acetate and proteinases. *J. Biol. Chem.* **270**, 18506-18511 (1995).

57. Vallon, R., Müller, R., Moosmayer, D., Gerlach, E. & Angel, P. The catalytic domain of activated collagenase I (MMP-1) is absolutely required for interaction with its specific inhibitor, tissue inhibitor of metalloproteinases-1 (TIMP-1). *Eur. J. Biochem.* **244**, 81-88 (1997).

58. Jones, G.C., Vankemmelbeke, M.N. & Buttle, D.J. Expression of recombinant ADAMTS in insect cells. *Methods Mol. Biol.* **622**, 83-98 (2010).

59. Chavaroche, A. et al. Glycosylation of a disintegrin and metalloprotease 17 affects its activity and inhibition. *Anal. Biochem.* **449**, 68-75 (2014).

60. Wong, E., Maretzky, T., Peleg, Y., Blobel, C.P. & Sagi, I. The Functional Maturation of A Disintegrin and Metalloproteinase (ADAM) 9, 10, and 17 Requires Processing at a Newly Identified Proprotein Convertase (PC) Cleavage Site. *J. Biol. Chem.* **290**, 12135-12146 (2015).

61. Prosise, W.W. et al. Protease domain of human ADAM33 produced by *Drosophila S2* cells. *Protein Expr. Purif.* **38**, 292-301 (2004).

62. Overall, C.M. & Lopez-Otin, C. Strategies for MMP inhibition in cancer: innovations for the post-trial era. *Nat. Rev. Cancer* **2**, 657-672 (2002).

63. Craig, V.J., Zhang, L., Hagood, J.S. & Owen, C.A. Matrix metalloproteinases as therapeutic targets for idiopathic pulmonary fibrosis. *Am. J. Respir. Cell. Mol. Biol.* **53**, 585-600 (2015).

64. Sari, D. et al. The MultiBac Baculovirus/Insect Cell Expression Vector System for Producing Complex Protein Biologics. *Adv. Exp. Med. Biol.* **896**, 199-215 (2016).

65. Sari-Ak, D. et al. VLP-factory and ADDomer: Self-assembling Virus-Like Particle (VLP) Technologies for Multiple Protein and Peptide Epitope Display. *Curr. Protoc.* **1**, e55 (2021).

FIGURES AND LEGENDS

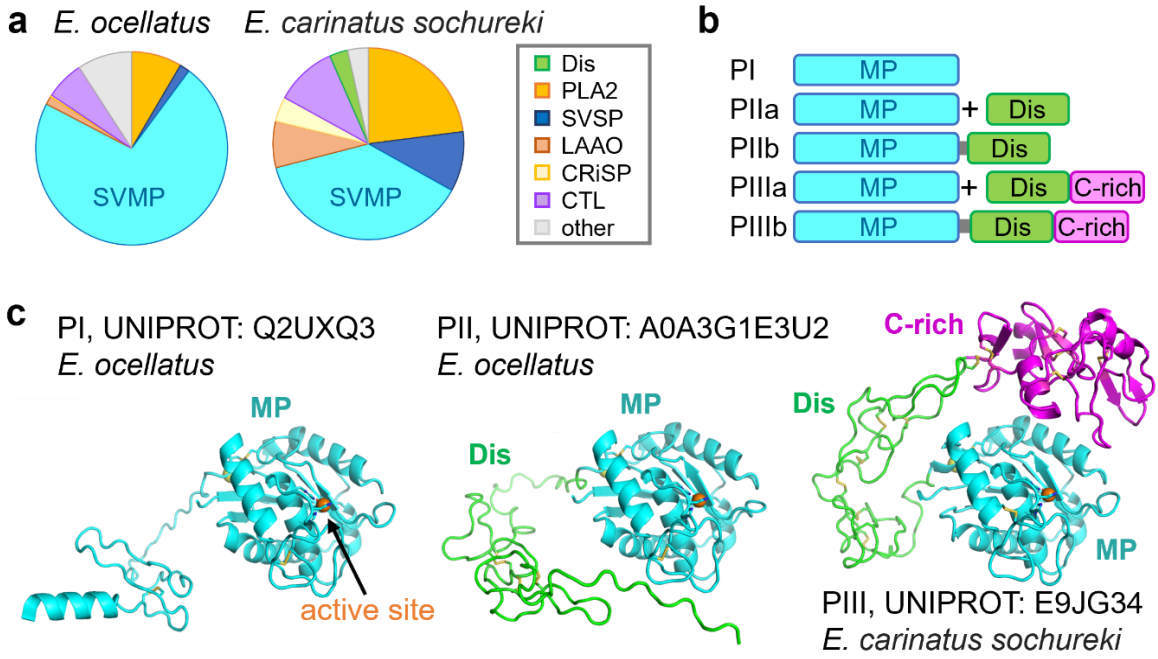

Figure 1: SVMP classification and abundance in *Echis* venom. (**a**) Pie charts displaying *Echis ocellatus* and *Echis carinatus sochureki* venom composition, with SVMP coloured in cyan[3]. (**b**) Simplified schematic of mature PI, PII and PIII SVMP architecture, showing metalloproteinase domain (MP, cyan), disintegrin domain (Dis, green) and cysteine-rich domain (C-rich, magenta). (**c**) AlphaFold 2 predicted structural models of PI and PII SVMPs from *Echis ocellatus*, and PIII SVMP from *Echis carinatus sochureki*. Domain names and colour coding as in panel b. Zn^{2+} ions in the active site are shown as spheres.

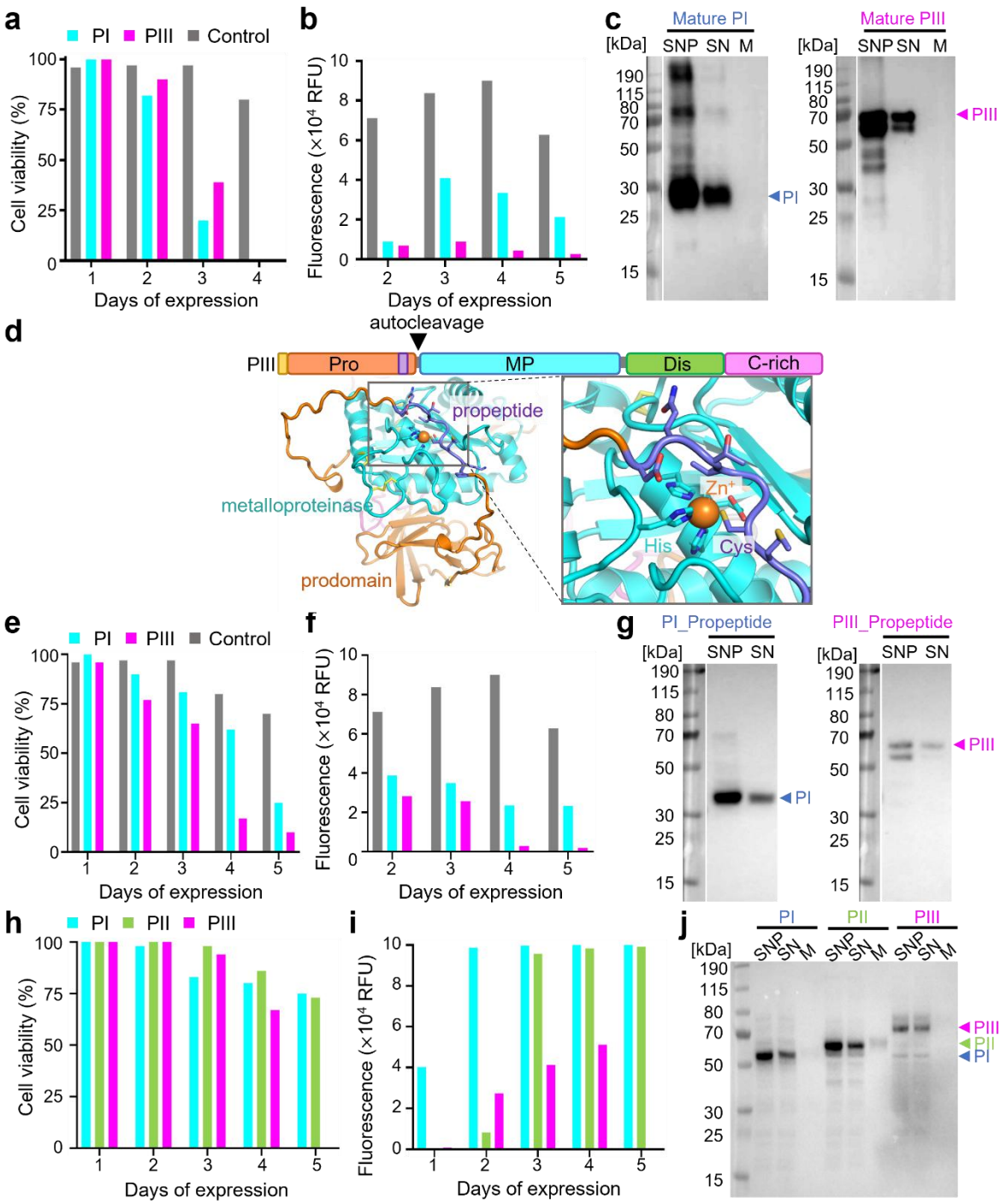

Figure 2: SVMP expression tests. Expression of mature SVMPs monitored by (**a**) cell viability, (**b**) YFP fluorescence, (**c**) Western blot analysis of His-tagged protein. (**d**) Above: Schematic of SVMP zymogen, with N-terminal prodomain (Pro, orange), propeptide (purple) and signal sequence (yellow). Below: left: AlphaFold 2[33] prediction of PI zymogen; right: zoom in on active site Zn^{2+} ion coordinated by histidines and propetide cysteine. Propeptide-SVMP-fusions expression monitored by (**e**) cell viability, (**f**) YFP fluorescence, (**g**) Western blot. SVMP zymogens

expression monitored by (**h**) cell viability, (**i**) YFP fluorescence (PIII harvested on day 4), (**j**) Western blot analysis. SNP: supernatant+pellet, SN: supernatant, M: media. Grey bars: non-toxic protein expression control, cyan: PI SVMP, green: PII SVMP, magenta: PIII SVMP.

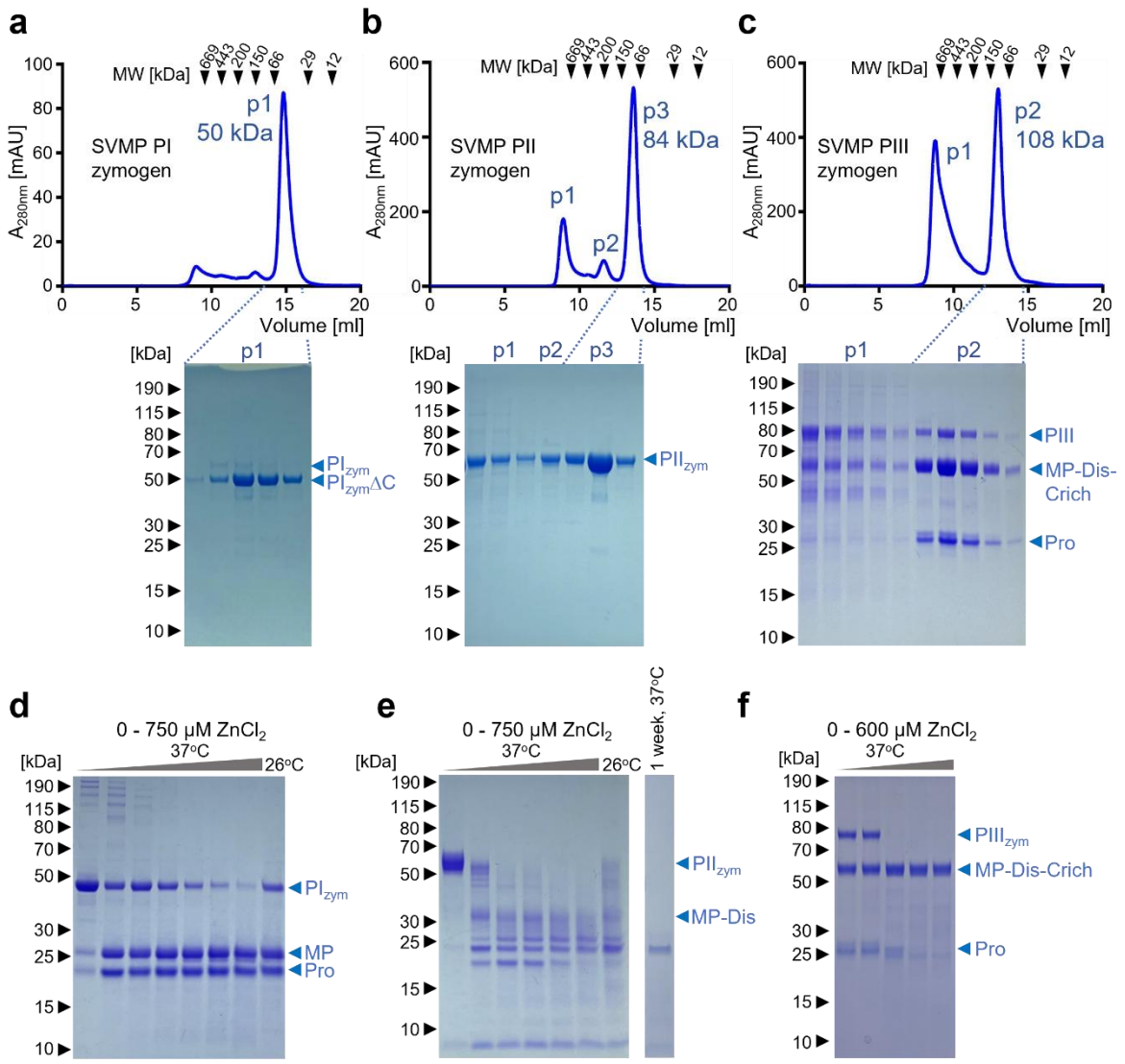

Figure 3: SEC Purification of SVMP zymogens after IMAC and IEX. Size exclusion chromatograms and SDS-PAGE of (**a**) PI zymogen ($PI_{zym}\Delta C$ lacks C terminal tags), (**b**) PII zymogen, and (**c**) PIII zymogen. $PIII_{zym}$ partial cleavage separate the prodomain (Pro) and the mature PIII. Elution volumes of MW calibration markers are indicated in the chromatograms as black arrows. (**d**) Activation of PI zymogen into metalloproteinase and prodomain. (**e**) Activation of PII zymogen into metalloproteinase-disintegrin and disintegrin domain (prodomain cannot be definitively identified). After 1 week only 8 kDa and 23 kDa bands remain. Control: incubation of SVMP zymogen at 26°C without Zn^{2+} addition. (**f**) Activation of PIII zymogen into prodomain and mature PIII. At higher Zn^{2+}concentrations, the prodomain is degraded.

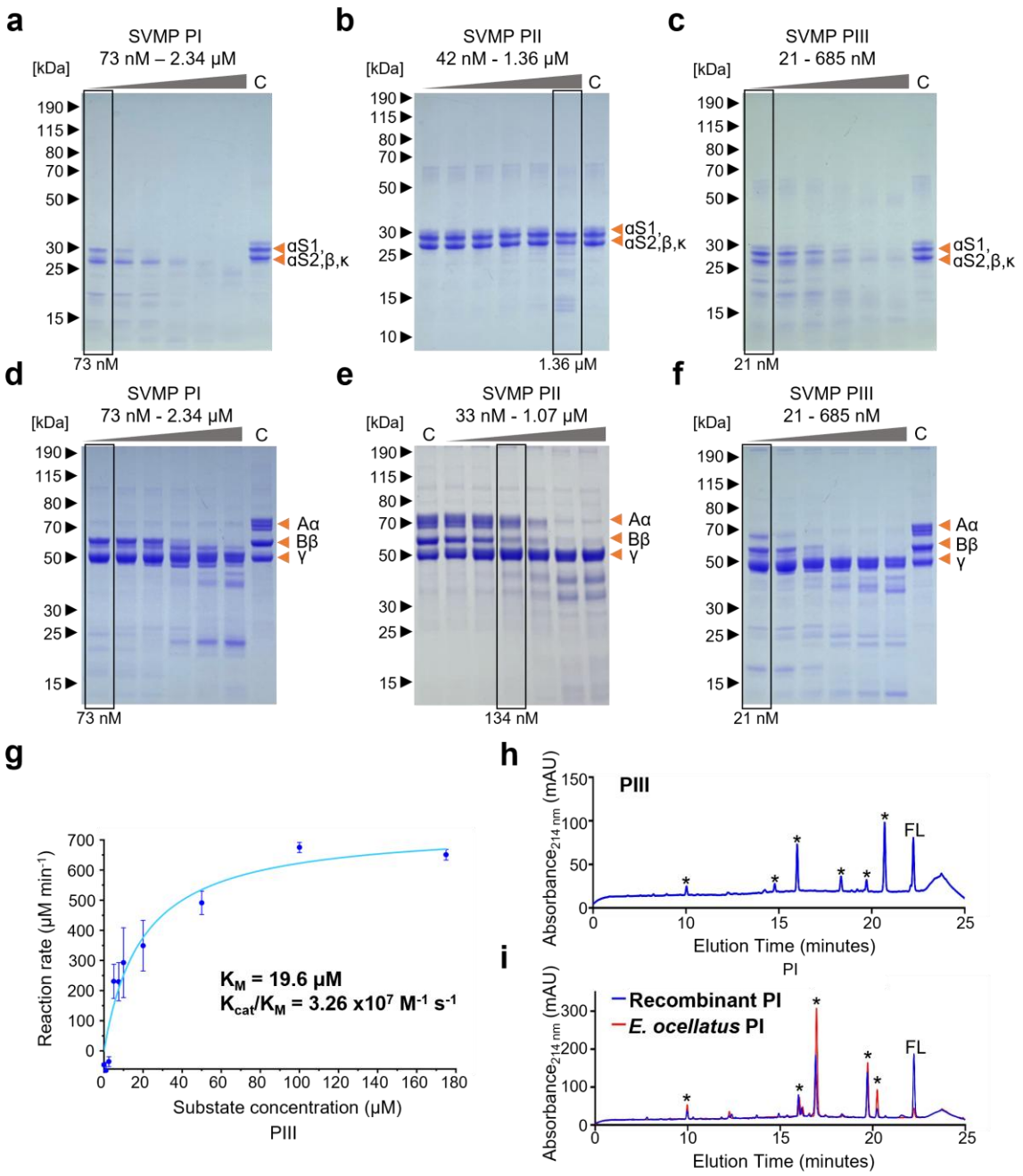

Figure 4: *In vitro* SVMP activity assays. Casein degradation in the presence of increasing amounts of (**a**) PI, (**b**) PII and (**c**) PIII SVMPs. Orange arrowheads: domains αS1, αS2, β and κ. Fibrinogen degradation in the presence of increasing amounts of (**d**) PI, (**e**) PII and (**f**) PIII. Orange arrowheads: fibrinogen chains Aα, Bβ and γ. C (control): incubation in the presence of 5 mM EDTA. (**g**) PIII SVMP activity towards the fluorogenic peptide substrate ES010. (**h,i**) Degradation of insulin B by (**h**) PIII and (**i**) recombinant (blue) and *Echis ocellatus* PI (red). Full-length insulin (FL) and degradation products (*) are marked above the peaks.

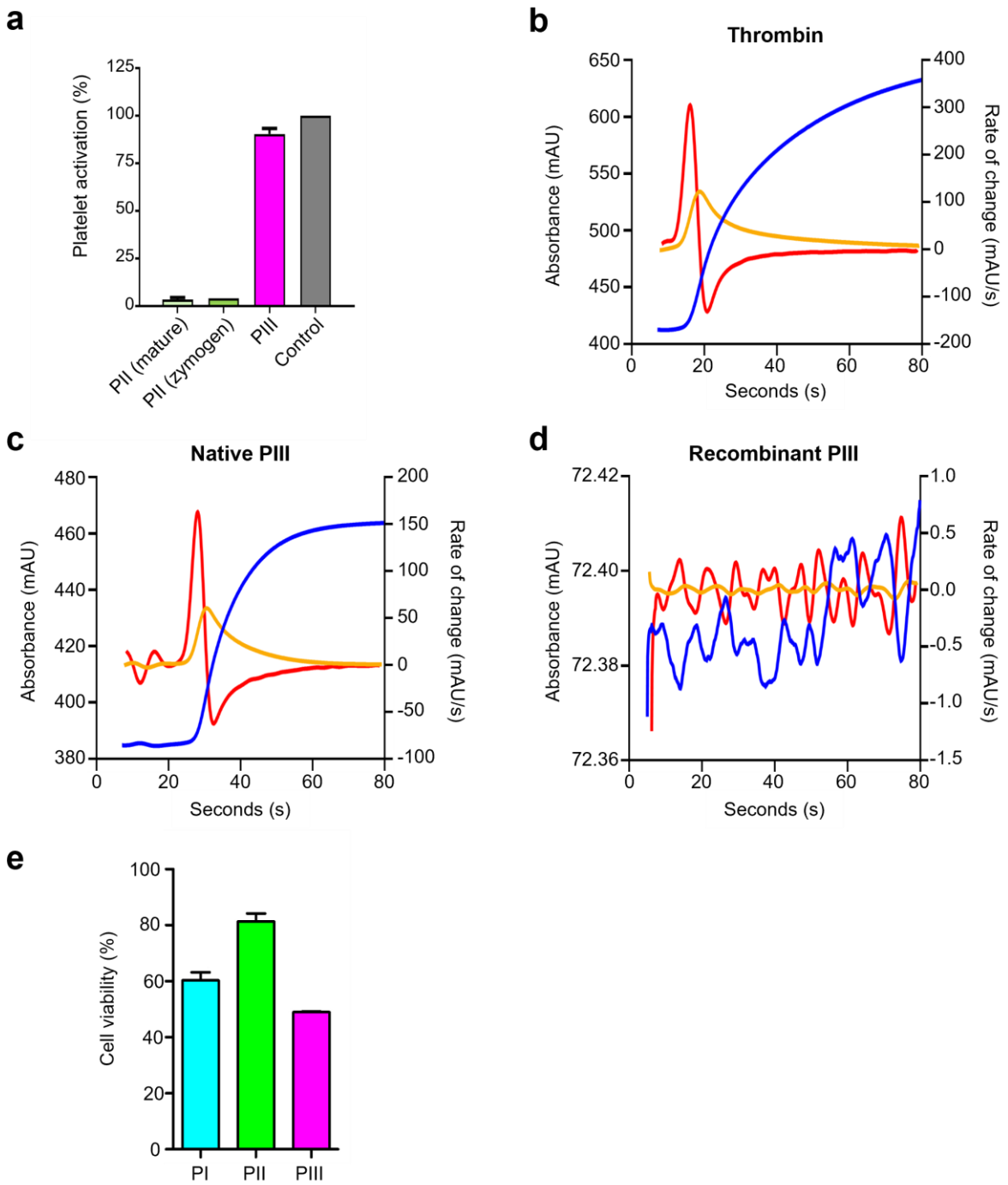

Figure 5: SVMP coagulation, platelet aggregation and cytotoxicity assays. (**a**) Inhibition of platelet activation by PII (mature and zymogen) and PIII. Control: human platelet rich plasma. Thrombin clot time assays using the ACL TOP coagulation analyser. Citrated human blood was spiked with (**b**) thrombin, (**c**) a pool of native *Echis ocellatus* PIII SVMPs and (**d**) the recombinant PIII SVMP. Change in absorbance (blue) is plotted on the left Y axis, rate of change (1st derivative: orange;

2nd derivative: red) is plotted on the right Y axis. (**e**) MTT cytotoxicity assay showing viability of HaCaT cells after 24 hour incubation with activated PI, PII and PIII SVMPs.

SUPPLEMENTARY INFORMATION

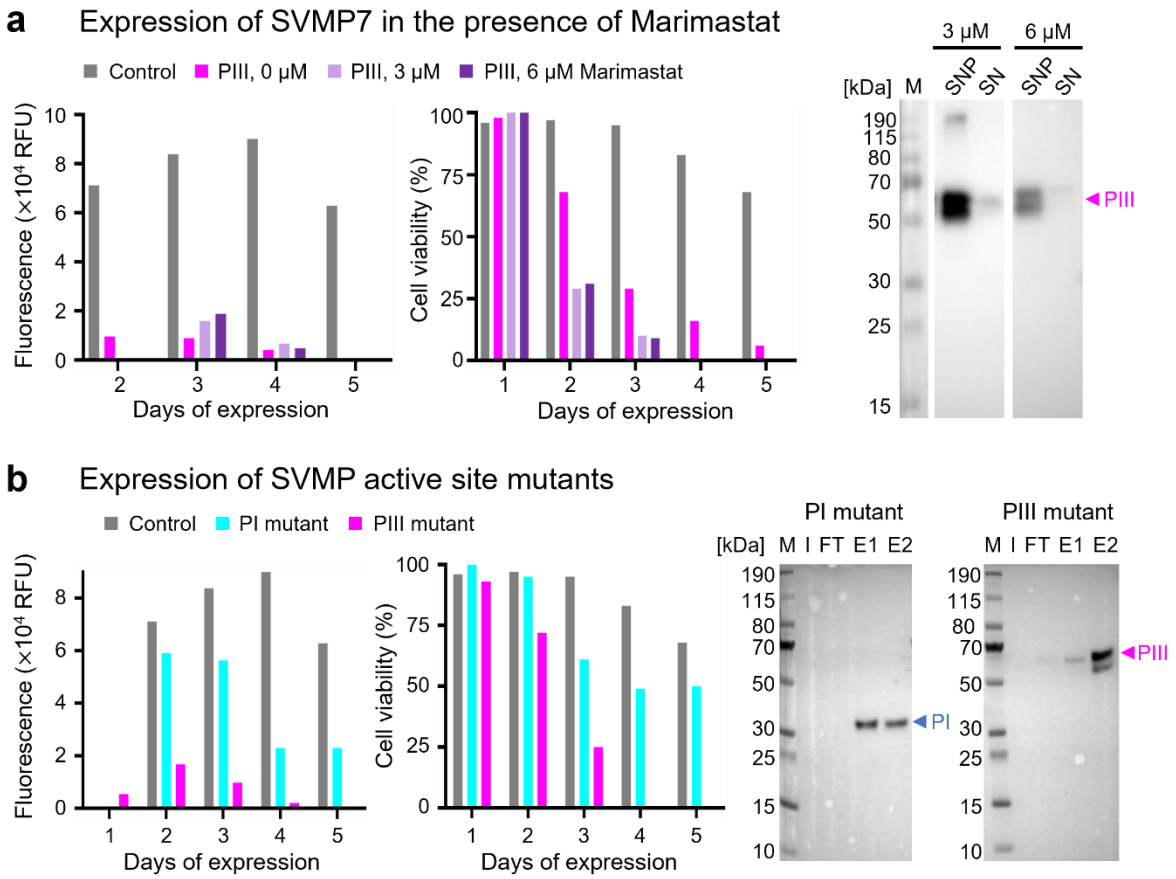

Supplementary Figure 1: SVMP expression tests using inhibitor and active site mutants. (**a**) Expression of PIII SVMP in the presence of 0 μM (magenta), 3 μM (lilac) or 6 μM (purple) Marimastat. Grey bar: non-toxic protein control expression. Expression is monitored by YFP fluorescence (left) and cell viability (middle). Right: Western blot analysis of expressed His-tagged protein. SNP: supernatant + pellet; SN: supernatant. (**b**) Expression of SVMP active site mutants monitored by YFP fluorescence (left) and cell viability (middle). Right: Western blot analysis of expressed His-tagged protein following Ni-NTA purification. I: input; FT: flowthrough; E1, E2: elution fractions.

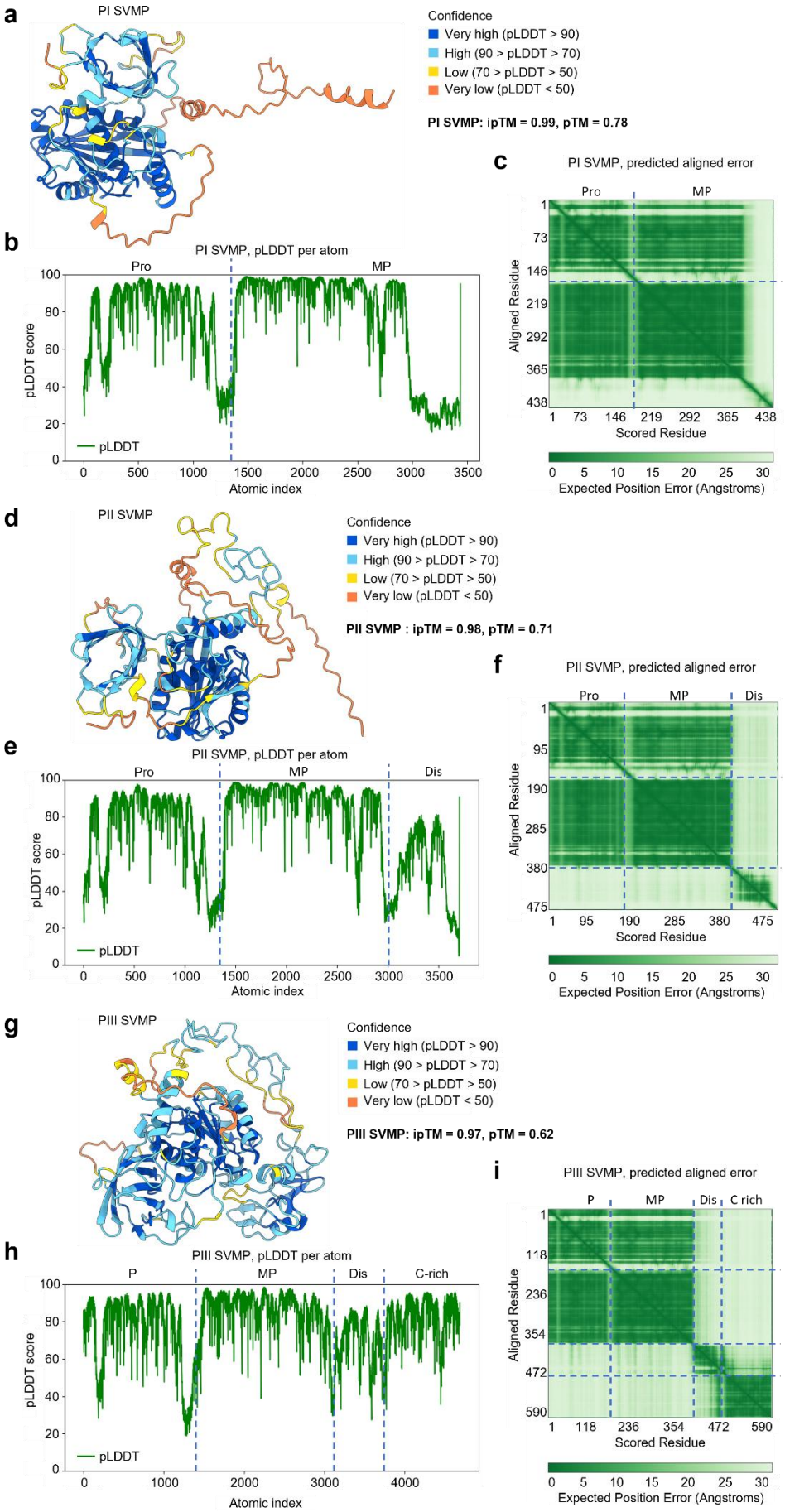
a
PI SVMP
Confidence
Very high (pLDDT > 90)
High (90 > pLDDT > 70)
Low (70 > pLDDT > 50)
Very low (pLDDT < 50)
PI SVMP: ipTM = 0.99, pTM = 0.78
b
PI SVMP, pLDDT per atom
Pro
MP
pLDDT score
pLDDT
Atomic index
c
PI SVMP, predicted aligned error
Pro
MP
Aligned Residue
Scored Residue
Expected Position Error (Angstroms)
d
PII SVMP
Confidence
Very high (pLDDT > 90)
High (90 > pLDDT > 70)
Low (70 > pLDDT > 50)
Very low (pLDDT < 50)
PII SVMP : ipTM = 0.98, pTM = 0.71
e
PII SVMP, pLDDT per atom
Pro
MP
Dis
pLDDT score
pLDDT
Atomic index
f
PII SVMP, predicted aligned error
Pro
MP
Dis
Aligned Residue
Scored Residue
Expected Position Error (Angstroms)
g
PIII SVMP
Confidence
Very high (pLDDT > 90)
High (90 > pLDDT > 70)
Low (70 > pLDDT > 50)
Very low (pLDDT < 50)
PIII SVMP: ipTM = 0.97, pTM = 0.62
h
PIII SVMP, pLDDT per atom
P
MP
Dis
C-rich
pLDDT score
pLDDT
Atomic index
i
PIII SVMP, predicted aligned error
P
MP
Dis
C rich
Aligned Residue
Scored Residue
Expected Position Error (Angstroms)

Supplementary Figure 2: Structural predictions of (**a**) PI, (**d**) PII and (**g**) PIII SVMP zymogens, performed by AlphaFold 3[33] in the presence of Zn^{2+}, along with the corresponding predicted Local Distance Difference Test (pLDDT) (**b, e, h**) and predicted Aligned Error (pAE) (**c, f, i**) plots.

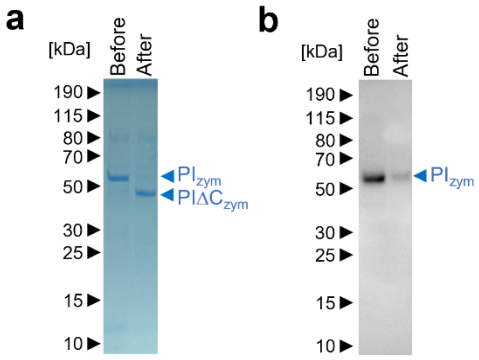

c

Protein FDR Confidence	Accession	Description	Coverage	# Peptides	# PSMs	# Unique Peptides	Area: F2: Sample	Score Sequest HT
High	**Q2UXQ3+tags**	**PI SVMP**	**59.591837**	**27**	**1087**	**27**	**8.532E+10**	**2337.7**
High	A0A7E5X2W4	La-related protein 1-like from *Trichoplusia ni*	16.224649	16	25	16	132016395	67.07
High	A0A7E5VL90	Adenylosuccinate lyase from *Trichoplusia ni*	43.699187	20	23	20	108915336	58.44
High	A0A7E5VKR1	Vacuolar proton pump subunit B from *Trichoplusia ni*	25.352113	11	15	11	53472561	36.55
High	A0A7E5WZM0	ATP synthase subunit alpha from *Trichoplusia ni*	26.391382	13	18	13	49168940	42.98

Supplementary Figure 3: PI SVMP characterisation before and after dialysis, following IMAC purification. (**a**) SDS-PAGE and (**b**) Western blot of His-tagged protein before and after dialysis, following IMAC purification. (**c**) Top 5 mass spectrometry hits of before dialysis sample. Keratin has been removed for simplicity.

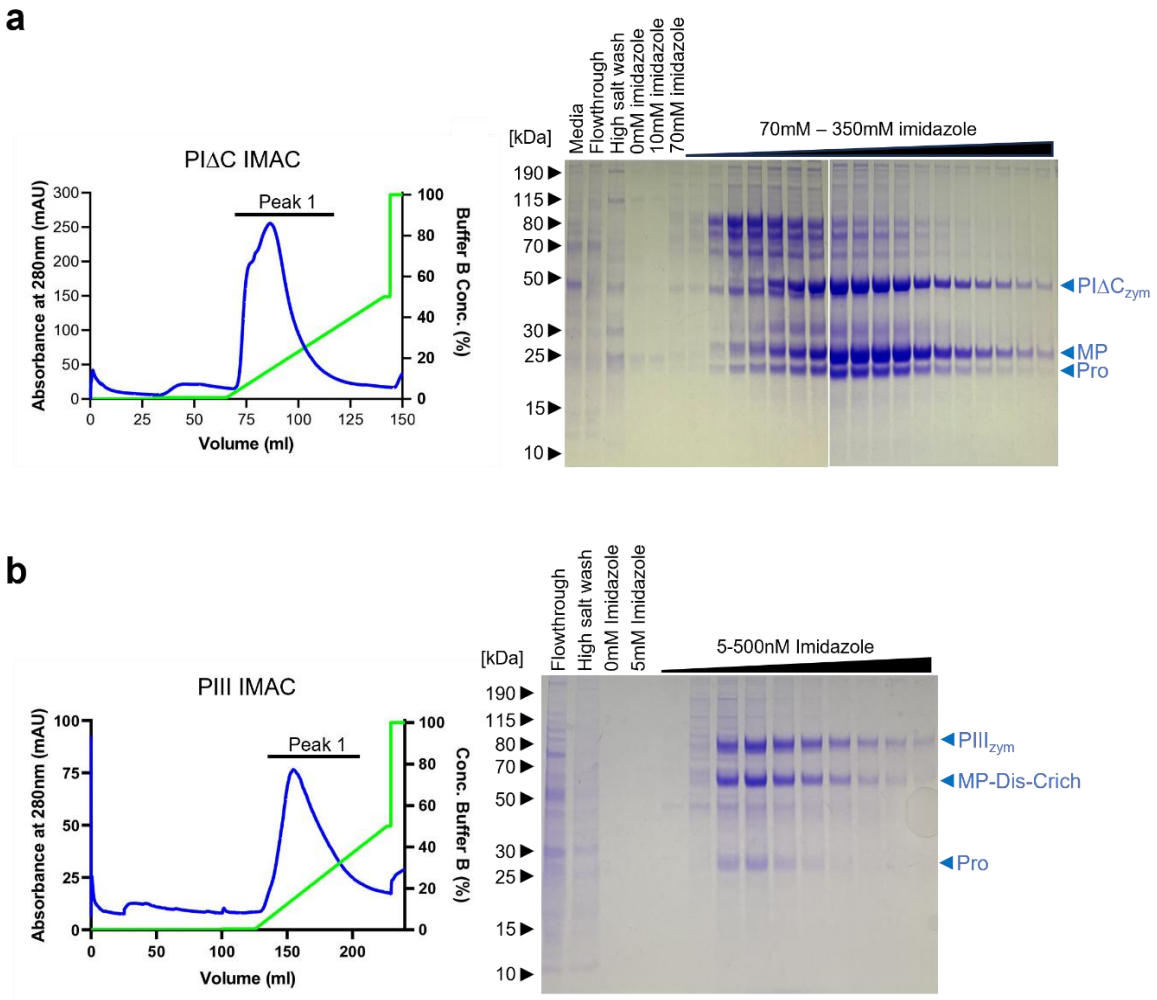

Supplementary Figure 4: IMAC Purification of secreted SVMPs from insect cell media. Non-reducing SDS-PAGE of IMAC purification of **(a)** PI SVMP (PIΔC) and **(b)** PIII SVMP.

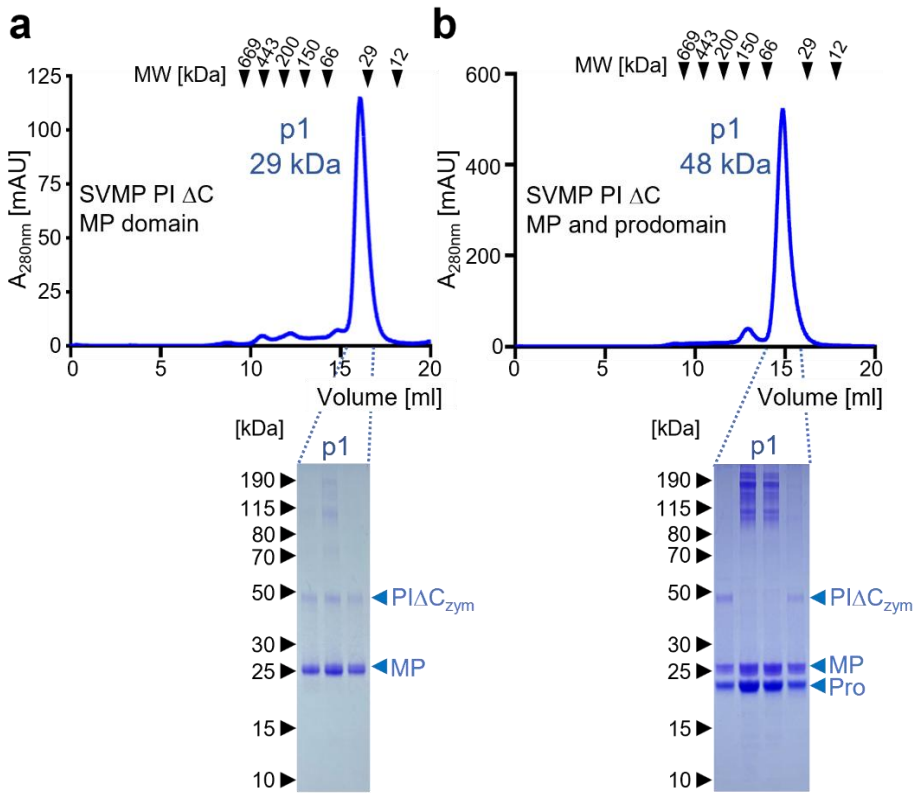

Supplementary Figure 5: SEC Purification of PI SVMP zymogen with shorter C terminus, following IMAC and IEX. Size exclusion chromatograms and SDS-PAGE of (**a**) metalloproteinase domain (MP) of PIΔC. (**b**) metalloproteinase domain (MP) and prodomain (Pro) of PIΔC.

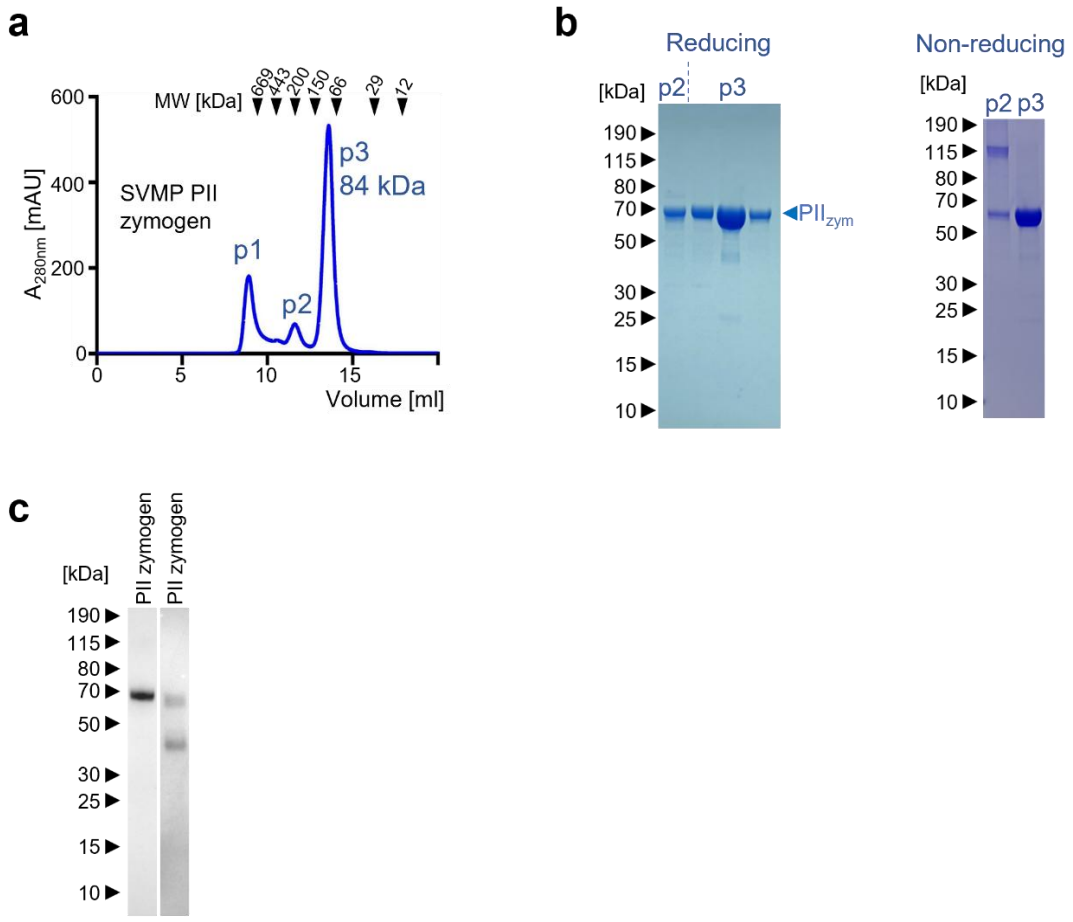

Supplementary Figure 6: SEC Purification of PII SVMP zymogen, following IMAC and IEX. (**a**) Size exclusion chromatogram and (**b**) reducing and non-reducing SDS-PAGE of SEC peaks 2 and 3. (**c**) Western blot analysis of His-tagged protein during activation of PII SVMP.

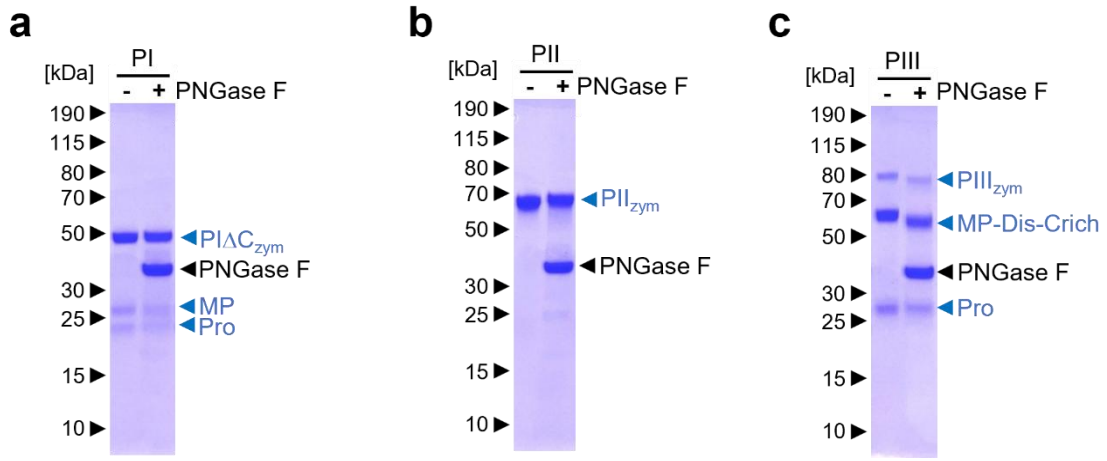

Supplementary Figure 7: Glycosylation test of recombinant SVMPs. Purified (**a**) PI, (**b**) PII and (**c**) PIII SVMP zymogens were treated with PNGase F. A shift to lower MW is observed in bands corresponding to PIII SVMP zymogen and mature PIII SVMP (MP-Dis-Crich).

a

Protein FDR Confidence	Accession	Description	Coverage	# Peptides	# PSMs	# Unique Peptides	Area: F4: Sample	Score Sequest HT
High	**sPDI**	**Snake venom protein disulfide isomerase**	**74.76**	**39**	**764**	**39**	**33529221181**	**1699.08**
High	**PIII SVMP**	**PIII SVMP**	**57.86**	**31**	**108**	**31**	**2499322340**	**308.03**
High	A0A7E5VVN0	T-complex protein 1 subunit delta from *Trichoplusia ni*	49.91	23	46	23	591351696	130.49
High	A0A7E5WZQ1	T-complex protein 1 subunit eta from *Trichoplusia ni*	54.23	24	48	24	560392602	125.74
High	A0A7E5X1U5	T-complex protein 1 subunit beta from *Trichoplusia ni*	60.82	29	60	29	498295832	158.19

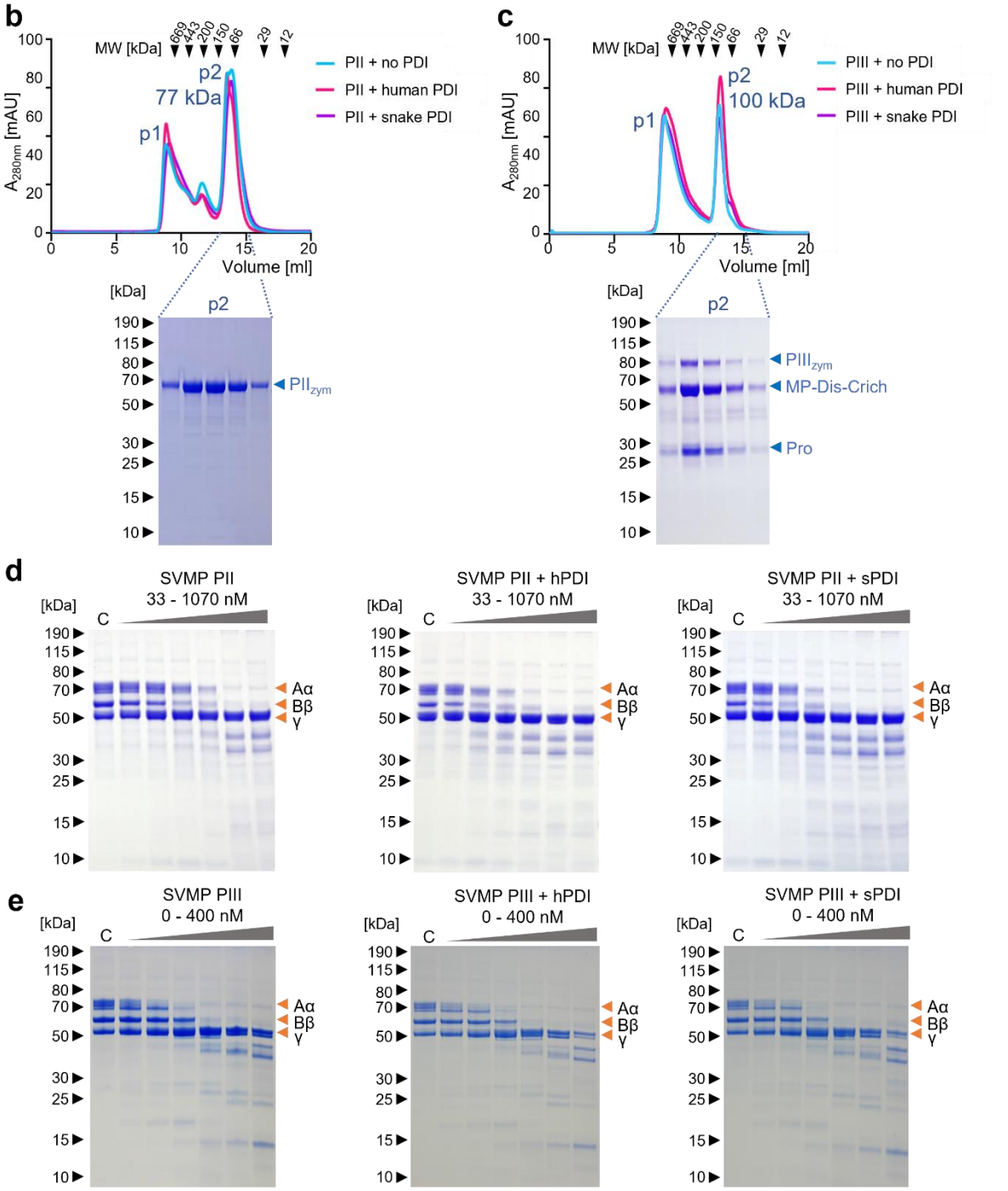

Supplementary Figure 8: SEC chromatograms of SVMPs produced in the presence and the absence of human and snake protein disulphide isomerases. (**a**) Top 5 mass spectrometry hits of PIII + sPDI IMAC flowthrough. Keratin and trypsin have been removed for simplicity. (**b**) PII SVMP zymogen and (**c**) PIII SVMP zymogen were co-expressed with human (magenta) or snake (purple) PDIs. SEC chromatograms were aligned with the control where no PDI was expressed (cyan). (**d**) Fibrinogen degradation assays in the presence of Zn^{2+} and increasing amounts of SVMPs PII, PII +hPDI (human PDI) and PII +sPDI (snake PDI). (**e**) Fibrinogen degradation assays in the presence of Zn^{2+} and increasing amounts of SVMPs PIII, PIII + hPDI and PIII + sPDI.

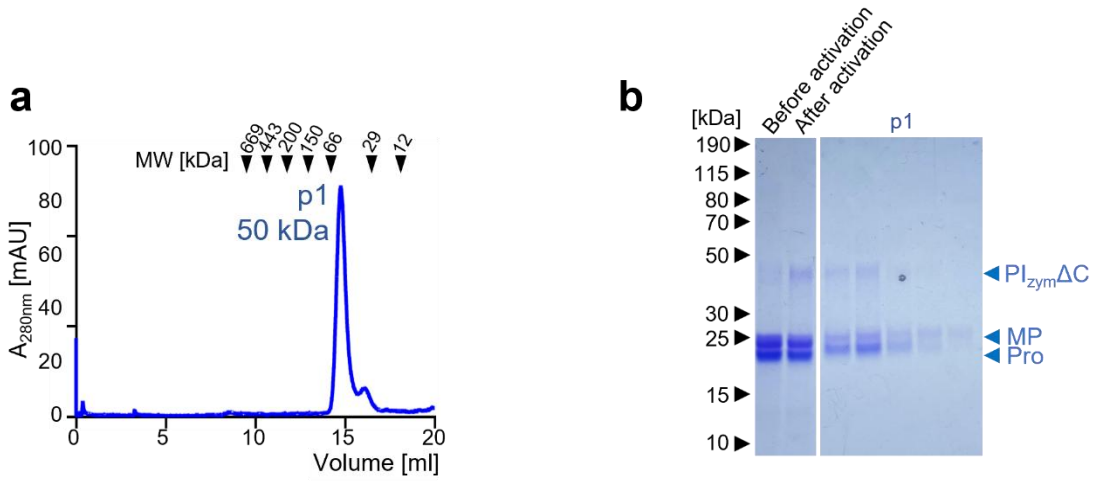

Supplementary Figure 9: Activated $PI_{zym}\Delta C$ SEC. (**a**) Size exclusion chromatogram and (**b**) corresponding Coomassie-stained SDS gel of activated $PI_{zym}\Delta C$, confirming metalloproteinase domain (MP) and Prodomain (Pro) remain bound together, despite the protein being active.